NACA TN No. 1675

# NATIONAL ADVISORY COMMITTEE FOR AERONAUTICS

TECHNICAL NOTE

No. 1675

## TEMPERATURE GRADIENTS IN THE WING OF A HIGH-SPEED AIRPLANE DURING DIVES FROM HIGH ALTITUDES

By Thorval Tendeland and Bernard A. Schlaff

Ames Aeronautical Laboratory,
Moffett Field, Calif.



Washington
July 1948

NATIONAL ADVISORY COMMITTEE FOR AERONAUTICS

TECHNICAL NOTE NO. 1675

# TEMPERATURE GRADIENTS IN THE WING OF A HIGH-SPEED AIRPLANE DURING DIVES FROM HIGH ALTITUDES

By Thorval Tendeland and Bernard A. Schlaff

## SUMMARY

Flight tests were undertaken to investigate the temperature gradients in the wing structure of a typical high-speed fighter airplane caused by rapid changes in surface temperatures. The tests consisted of measuring the temperatures of the structure throughout the wing during dives of the airplane from 35,000 to 5,000 feet, at rates of vertical descent up to 225 feet per second. The data are presented in the form of tables of the measured temperatures and plots of the temperature change of typical parts of the wing structure during the dives.

The tests showed that temperature gradients which are produced in an aircraft structure as a result of sudden changes in surface temperature are essentially a transient condition and, therefore, are determined mainly by the relative size of adjacent structural members, the thermal bond between these members, and the rate of change of surface temperature. Predicted and measured temperature differences between a spar cap and the adjacent skin in dives showed good agreement, and it is believed that the method used for predicting temperature gradients may be applied to other airplanes and dive conditions. Computations were made to show the effects of increases in (1) the rate of descent, and (2) structural mass distribution (thermal capacity) on the temperature distribution for dives at higher speeds. It was shown that a structural design employing a thin wing skin attached to a heavy spar cap is conducive to severe temperature gradients.

Exploratory calculations were made of the stresses resulting from temperature gradients. In spite of the fact the prediction of thermal stresses corresponding to observed temperature gradients is difficult and probably inaccurate at the present time because of the

lack of information on thermal stresses for typical aircraft construction, the calculations indicate that: (1) For airplanes similar to the test airplane, operated at approximately the test conditions, thermal stresses will be of minor importance; (2) the increased structural sizes required for higher performance airplanes will alleviate the thermal stress problem; and (3) the importance of the thermal stress problem depends upon the specific case.

## INTRODUCTION

With the advent of aircraft capable of flight in the transonic and supersonic speed ranges, several new problems are added to the field of structural design. One of these problems, which is the subject of this investigation, is the determination of the magnitude of thermal stresses which occur as a result of temperature gradients in the airplane structure. These temperature variations in the structure are the result of subjecting the outer surface of the airplane to rapidly changing temperature conditions which accompany dives from high altitudes, or by changes in the amount of friction heating produced by large changes in speed.

Both an increase in airplane speed and an increase in ambient-air temperature tend to raise the temperature of the boundary-layer air. The outer surfaces of the fuselage and the wing can be expected to react quickly to this change in temperature, since both the fuselage and the wing represent bodies of limited heat capacities with large surface areas in intimate contact with the boundary-layer air. In the case of the ribs and spars, however, it is obvious that the reaction to a change in boundary-layer temperature would be more sluggish, with the result that transient temperature gradients in the structure would exist for a short period of time. Since these temperature gradients are of a transient nature, the magnitude of the temperature differences will be determined by both the rate of change of the boundary-layer temperature and the over-all change in temperature of the boundary-layer air. Of the two conditions, the rate of change of the boundary-layer temperature can be expected to have as great, if not greater, influence on the magnitude of the temperature gradients.

Although it is readily evident why and how these temperature gradients can occur, the problem is to determine the conditions under which these gradients will reach sufficient magnitude to produce thermal stresses requiring consideration in the structural design. The purpose of this investigation was to measure the

magnitude of the thermal gradients in the wing of a typical high-speed fighter airplane during dives and to provide a basis for the prediction of the gradients to be anticipated in aircraft of higher performance.

Methods for calculating the temperature rise of a surface in high-speed flight are presented in references 1 and 2. These procedures are not directly applicable to present day aircraft structures unless some reasonable assumption can be made for the flow of heat into the interior of the structure.

Correlation between observed or estimated temperature gradients and the resultant thermal stresses is very difficult because of the limited test data available on the subject and because of the fact that the intricacies of an aircraft structure are not readily amenable to the analytic approach. Flight measurements of thermal stresses in a wing caused by operation of a thermal ice-prevention system are presented in reference 3. The results of reference 3 have been used in this report to predict the pattern of the thermal stresses which would be induced in the wing during a dive.

The flight tests were conducted at the Ames Aeronautical Laboratory, Moffett Field, Calif.

## DESCRIPTION OF EQUIPMENT

The airplane used to conduct the tests is shown in figure 1. A sketch of the wing construction is shown in figure 2. The wing is of all-metal stressed-skin construction with the main spars located at 20 percent and 52 percent of the wing chord. An auxiliary spar is located at 75 percent of the wing chord. The skin is heavily reinforced between the two main spars with extruded T and H sections on the upper surface and with angle sections on the lower surface. Aft of the 52-percent-chord main spar, and on the nose section, the skin is stiffened in a chordwise direction with corrugated sheets.

To investigate the temperature lag of the structure adjacent to large masses of cold fuel, an integral fuel tank was built into the right wing of the airplane. The fuel tank was bounded by the 20-percent and the 52-percent spars, the upper and lower surfaces of the wing, and by specially installed solid ribs at stations 141 and 164.

## DISCUSSION

### Temperature Gradients

The temperatures of representative components of the wing structure during the dives are shown in figures 5 to 9. Figure 10 presents the chordwise distribution of the surface temperature at the termination of the three dives. The data for these figures were taken from table I. Curves of stagnation temperature (free-air temperature plus full kinetic temperature rise) have been added to figures 5 to 9 for comparative purposes.

The curves of figures 5 to 9 indicate that, in general, the time at which the maximum temperature difference occurred was during the pull-out from the dives or shortly thereafter. As a result of this condition, it is evident that the induced thermal stresses would be a maximum when the stresses from aerodynamic loads would be large. As might be expected, since temperature gradients in the structure are a result of thermal lag, the curves show the temperature differences to be a function of two factors: namely (1) the rate of descent of the airplane, which is the primary factor controlling the rapidity of the temperature changes imposed on the airplane surfaces; and (2) the distribution of mass in the structure, which results in differences in thermal capacity of adjacent parts.

The influence of the rate of descent on the structural temperature differences is indicated by the observed maximum temperature differences between the lower flange of an H section and the skin, as shown in figure 6. This figure shows that for average rates of vertical descent of 73, 150, and 225 feet per second, during which an over-all ambient temperature change of approximately 125° F was imposed on the airplane in 6.8, 3.3, and 2.2 minutes, respectively, the resulting maximum temperature differences were 20°, 25°, and 37° F, respectively. From a consideration of the extremes, it is evident that tripling the rate of vertical descent almost doubled the temperature difference. As shown in figure 4, the kinetic heating, as represented by the difference between the ambient-air temperature and stagnation temperature, was of minor importance in comparison with the change in the ambient-air temperature. The maximum kinetic temperature rises were of the order of 35° to 40° F, as compared to the 125° F temperature change resulting from change of altitude.

The effect of mass distribution (variation of thermal capacity) on the temperature gradients can be observed by a study of figures 5 to 10, which present the following combinations:

Layers of paint on the surface of a high-speed airplane or missile have been shown to have an appreciable effect on the rate at which the temperature of the surface under the paint approaches the temperature of the boundary-layer air. To investigate this effect, a layer of paint approximately 0.046 inch thick was applied to the left-wing surface at station 112. This heavy coat of paint simulates a filler which might be used on future high-speed aircraft to obtain surface smoothness.

The locations of the thermocouples throughout the wing structure are shown in figure 3. Selection of the thermocouple locations was based on anticipated temperature differences occurring as a result of lag in heat flow across the main structural members and as a result of differences in masses of adjacent components of the structure. The thermocouples used to measure skin temperatures were strip-type iron-constantan thermocouples rolled to a thickness of approximately 0.002 inch. These thermocouples were cemented to the skin and then sprayed with a thin layer of paint to obtain a smooth surface. In the case of the thick layer of paint on the left wing at station 112, a thermocouple was installed on each side of the paint layer (fig. 3(e) ). For the internal structure of the wing, strip and rivet-type thermocouples were used. The rivet thermocouples were imbedded in structural rivets.

All temperature readings of the structure were recorded with two self-balancing potentiometers. Standard NACA instruments were used to measure airspeed, free-air temperature, and altitude.

## PRECISION OF MEASUREMENTS

An exact determination of the over-all accuracy of the temperature measurements was not possible, due to the effect of lag in the thermocouple response when measuring rapidly changing temperatures. However, this effect is believed to be small. Of the most interest are the temperature differences between two or more components of the structure as recorded at a given time. The effects of lag in determining the temperature differences would be of minor importance, since each temperature measurement would lag approximately the same amount. Validity of indication of the two types of thermocouples was checked by installing both types of thermocouples at approximately the same location on the skin. Both types of thermocouples indicated temperatures within $1^{\circ}$ F of each other throughout the dive tests. The accuracy of the indication of the potentiometers was checked during the dive tests by recording a known reference temperature. This error was found not to exceed $\pm 2^{\circ}$ F.

Ambient-air temperatures were evaluated from data taken at intervals of level flight during the ascent of the airplane. This was necessary because of an appreciable lag in the installation to measure free-air temperature during the dives. The corrections to the free-air-temperature measurements for kinetic heating were evaluated from a flight calibration of the free-air-temperature installation. The values presented for ambient-air temperature are estimated to be accurate to $\pm 4^{\circ}$ F.

The airspeed measurements were corrected from a flight calibration of the airspeed installation. The airspeed data are considered accurate to $\pm 1\text{-}1/2$ percent.

## TEST PROCEDURE AND RESULTS

For each dive test, the airplane was climbed to 35,000 feet pressure altitude, with readings of ambient-air temperature being recorded by the pilot at intervals of 5,000 feet. At 35,000 feet the airplane was cruised at an indicated airspeed of about 150 miles per hour for 15 minutes to allow the structure to achieve an equilibrium temperature. The pilot then started the recording instruments and dived the airplane to a pressure altitude of 5,000 feet. During each dive, an attempt was made to hold the rate of vertical descent approximately constant throughout the dive.

Time histories of true airspeed, altitude, and free-air temperature during four representative dives are shown in figure 4. The free-air-temperature data presented are corrected for kinetic heating.

The temperatures of the structure as measured during the four dives of figure 4 are presented in table I. A different value of time must be presented for each temperature because the recording instrument selected the thermocouples in rotation. The letters preceding the thermocouple numbers in table I correspond to the type of thermocouple as designated in figure 3. The discontinuities in the numbering system in table I are the result of omitting thermocouples which failed during the tests and of omitting thermocouples, the locations of which were not considered of sufficient importance to include in the report. The data as presented in table I during flight 4 include only temperatures as measured for the fuel and the structure surrounding the fuel. These data were included because this was the only flight for which temperatures were obtained for the fuel at the center of the fuel tank.

1. Skin and stiffener (fig. 5)
2. Skin and former (fig. 6)
3. Across a rib (fig. 7)
4. Spar cap and spar web (fig. 8)
5. Fuel and structure of fuel tanks (fig. 9)
6. Skin and spar cap (fig. 10)

On the test airplane, the maximum-temperature differences occurred between the skin and the spar caps (fig. 10). The dips in the curves at the spar locations indicate clearly the thermal lag associated with surface areas connected to large masses. The curves for thermocouples S1 and M2 in figure 8 show that the rates of temperature rise of the inner and outer surfaces of the spar cap at the 20-percent chord are almost identical, indicating good heat transfer from the surfaces. Because of the mass of the spar caps, however, the temperature lags behind that of the adjacent skin by some 30° to 40°, as shown in figure 10.

The mass distribution causing the second largest temperature differences in the wing was that associated with the large masses of fuel in the wing. As may be noted from figure 9, the temperature of the fuel during the dive increased only slightly, while the temperature of the skin rose rapidly and the temperature of the stringer immersed in the fuel assumed an intermediate position. Some indication of the effect of the presence of the cold fuel on the temperature difference between the skin and the stringer can be obtained by a comparison of the data in figure 9 with those for a similar structural configuration and dive without the presence of fuel (fig. 5(b)). The temperature difference between the skin and the stringer at the end of the dive is seen to be about 10° F without fuel and 20° F with fuel. The fuel would have had even greater influence on the temperature difference between the skin and the stringer had time been allowed before the dive for the fuel temperature, which was about 20° F at the start of the dive, to approach more closely the ambient-air temperature of -60° F.

A factor which would have a modifying influence on the temperature differences as previously discussed, is the insulating properties of a relatively thick layer of paint. The magnitude of this factor is indicated in figure 11 by the difference between the skin temperature and surface temperature when the surface is coated with such a layer of paint. The temperature difference was found to be approximately 20° F at the termination of the dive at the highest rate of vertical descent. It is of interest to note that the insulating action of the paint was sufficient to produce a

greater temperature drop through the paint than existed between the skin and the adjacent stringer. This fact would suggest that, for the transient condition, both thermal stresses and undesirable high surface temperatures can be alleviated by the use of paint.

In an attempt to arrive at some means of generalizing the foregoing results, a comparison has been made of the experimental temperature differences between the spar cap and the adjacent skin and the computed differences based upon simplifying assumptions. The skin and spar-cap region selected for the comparison was the upper surface of the right wing at 20 percent of the wing chord, station 76 (fig. 3(a) ). A sketch of the skin and spar cap is shown in figure 12. The calculation procedure employed was to set up equations which represented the heat flow for the spar cap and the adjacent skin for any time increment, and then to solve the equations by a step-by-step solution from the start to the end of the dive. The equations and the assumptions involved in their solution are discussed in the appendix of this report.

The calculated skin and spar-cap temperatures for flights 1, 2, and 3 are compared with the observed values in figure 13. At the termination of the dives, the calculated temperatures are somewhat higher than the measured temperatures, but of most interest is the temperature difference between the skin and the spar cap. The calculated temperature differences between the skin and the spar cap at the end of the dives $\Delta t$, in figure 13, are in good agreement with the measured temperature differences, and the method provides a means for predicting the temperature differences to be anticipated for arrangements and dives beyond the scope of the present tests.

To obtain an indication of the effects of increases in the rate of descent and also changes in the mass of the structure on the temperature gradients, calculations have been made for three different size skin and spar-cap combinations for a rate of vertical descent range from 200 to 1100 feet per second. One of the three designs selected corresponded to the test airplane spar-cap and skin combination previously analyzed (figs. 12 and 13) and the remaining two designs were similar but larger to correspond to the probable sizes required for strength at higher diving speeds. For rates of vertical descent in which the speed of the airplane would be in the transonic and supersonic regions, the airfoil section was assumed to be diamond shaped with a wedge angle at the leading edge of $8^{\circ}$. The location of the spar cap with respect to the leading edge was assumed to be the same as that on the wing of the test airplane.

The calculated temperature differences for the three skin and spar-cap arrangements are presented in figure 14 for dives from 35,000 feet to 5,000 feet. An examination of figure 14 indicates that, at high rates of vertical descent, a skin and spar-cap combination such as that on the test airplane (curve A) would experience an appreciable temperature difference. However, if both the skin and the spar cap are increased in mass, a reduction in temperature difference results. This effect is indicated by curves B and C. The reduction in temperature difference is due to the increased heat capacity of the thicker skin and also to the increased cross-sectional area of the skin available for heat flow. Thus, it is seen that the increased structural mass required for strength at the higher diving speeds tends to compensate for the increased rate of boundary-layer temperature rise resulting from aerodynamic heating and change of altitude. Whether or not this compensation will be adequate to eliminate entirely the problem of thermal stresses depends upon the particular airplane and the conditions of the dive. The method of calculation presented in this report provides a simple means for computing, at least for the single case of a skin and spar-cap combination, the approximate magnitude of the temperature differences to be expected.

Of considerable interest with regard to the curves, shown in figure 14, would be comparisons between the predicted values and actual test data for the various skin and spar-cap combinations. One possibility for obtaining such test data and also as a suggestion for future research would be to heat the surfaces of a typical structural arrangement by means of heating pads or lamps. The amount of heat applied to the surface could be varied to obtain rates of changes of the surface temperature similar to those encountered in flight. Temperature gradients throughout the structure could then be readily measured. This test procedure has an advantage over the analytical approach because it eliminates the uncertainty associated with the assumption of a perfect thermal bond between the components of the structure.

## Thermal Stresses

The evaluation of the actual thermal stresses induced in a wing structure as a result of temperature gradients is a difficult problem. This is partially due to the fact that a wing structure is not a rigid body and, consequently, some movement between the structural components may occur and thus relieve some of the thermal stresses. However, an indication of the thermal stresses induced in the wing of the test airplane was obtained by comparing the temperature

gradients found in this investigation with the temperature gradients and resultant thermal stresses observed in reference 3. In this investigation, heated air was supplied to the leading edge of the wing of a large twin-engine transport airplane and the temperatures and stresses of the wing were measured at various positions on the chord at two wing stations. As a result of the relatively warm leading edge tending to expand, compression stresses were induced in this portion of the wing, while tension restraining forces were generated immediately aft of the leading-edge heated region.

As may be noted in figure 10, the skin panels at the leading edge and between the two main spars were relatively warm as compared to the two main spars. Therefore, on the basis of the stress pattern found in reference 3, it seems reasonable to conclude that, considering only the thermal stresses, the skin panels would be in spanwise compression, while the spars would be in spanwise tension. A first approximation of the compression stress in the skin can be made by assuming the skin area $S_s$ to be completely restrained from expansion by the spar cap and the rest of the wing structure. (See sketch of the skin and spar-cap junction in fig. 12.) If it is assumed there is no buckling action, the compression stress in the skin for complete restraint $f_{s_r}$ can be readily calculated for any observed temperature difference between the skin and the spar cap. In the actual case, the value of $f_{s_r}$ would be reduced by the fact that the spar cap would elongate somewhat. For the purpose of this report, the assumption was made that the actual stress in the skin $f_s$ and the spar cap $f_c$ would be related to the completely restrained skin stress $f_{s_r}$ as follows:

$$f_s = \frac{y_c - y_s}{y_c} f_{s_r}$$

and

$$f_c = \frac{y_s}{y_c} f_{s_r}$$

where $y_s$ and $y_c$ are the thickness of the skin and spar cap, respectively, as shown in figure 12.

Based on the foregoing assumptions, the calculated stresses in the spar cap and the adjacent skin, at wing station 76 of the test airplane, are presented in figure 15. The computed stresses, as shown by the data points in figure 15, were calculated from the temperature difference between the skin and the spar cap as found at the termination of the dive in flight 1. The tension stresses are the stresses in the spar cap and the compression stresses are the stresses in the skin. The basis for fairing the stress curve in figure 15 was the pattern of the thermal stresses which was found to occur in the heated wing in reference 3. The chordwise temperature distribution curve upon which the computations are based and which is shown in figure 15 is the same as the curve shown in figure 10 for flight 1, with the exception of the spar-cap temperatures. The spar-cap temperatures, which are indicated by the dips in the curve, are the average temperatures between the upper and lower surfaces of the spar caps.

As shown in figure 15, the maximum compression stress in the skin is seen to be of the order of 6,000 pounds per square inch, and occurs at the rear spar cap. For the test airplane, a compression stress in the skin of this magnitude is not considered critical. In future aircraft, the induced thermal stresses may merit careful consideration, depending upon the flight conditions and the design of the wing structure.

## CONCLUSIONS

Based upon a consideration of observed temperature gradients which occurred in the wing of a high-speed fighter airplane during dives from 35,000 feet to 5,000 feet, it is concluded:

1. Temperature gradients which are produced in an aircraft structure as a result of sudden changes in the surface temperatures are essentially a transient condition, and as such are determined mainly by the relative size (thermal capacity) of adjacent structural members and the rate of change of surface temperature. The thermal bond between adjacent structural members would be an influencing factor.

2. For airplanes similar to the test airplane and subjected to dives of the same order of rate of vertical descent, the temperature gradients and thermal stresses will be appreciable but of secondary importance as compared to stresses due to aerodynamic loads.

3. For structural arrangements and flight conditions beyond the scope of these tests, the seriousness of the thermal stress problem will be dependent upon the specific airplane and operational conditions. Exploratory calculations indicate that the increased structural sizes required at increased diving speeds will greatly alleviate the temperature gradient problem.

4. The order of magnitude of the temperature gradients between adjacent components of the structure can be calculated, provided a reasonable assumption of the degree of thermal bond between the components can be made. In the present analysis, the assumption of perfect thermal bond provided good agreement between calculated and observed values.

5. The evaluation of the thermal stresses generated in an aircraft structure by the existence of thermal gradients is difficult and probably inaccurate at the present time. The recommendation is made that further data be obtained to enable a more complete evaluation of thermal stresses.

Ames Aeronautical Laboratory,
National Advisory Committee for Aeronautics,
Moffett Field, Calif.

## APPENDIX

The method used to determine the skin and spar-cap temperatures was to establish a heat balance for a unit spanwise length of the spar cap and a unit spanwise length of the skin adjacent to the spar cap. The equations determined in this manner were then solved simultaneously for short intervals of time in a step-by-step manner throughout the dive for the skin and spar-cap temperatures. A sketch of the skin and spar cap is shown in figure 12 in order to assist in interpreting the equations for the heat flow to the skin and the spar cap. The equation used for heat flow to the spar cap was

$$\tau h S_c (t_a - t_{c_2}) + \frac{2\tau k A (t_{s_2} - t_{c_2})}{l} = W_c \, c_p \, (t_{c_2} - t_{c_1}) \qquad (A1)$$

and for the skin

$$\tau h S_s (t_a - t_{s_2}) - \frac{\tau k A (t_{s_2} - t_{c_2})}{l} = W_s c_p (t_{s_2} - t_{s_1}) \qquad (A2)$$

The symbols and subscripts used in equations (A1) and (A2) and the symbols shown in figure 12 are defined as follows:

| | |
|---|---|
| A | cross-sectional area of the skin for heat flow, square feet |
| $c_p$ | specific heat, Btu per pound, $^{\circ}F$ |
| h | surface heat-transfer coefficient, Btu per hour, square foot, $^{\circ}F$ |
| k | thermal conductivity of aluminum, Btu per hour, square foot, $^{\circ}F$ per foot |
| l | distance for heat flow between skin and spar cap, feet |
| S | heat-transfer surface area, square feet |
| t | temperature, $^{\circ}F$ |
| W | weight of material, pounds |
| $\tau$ | interval of time, hours |

Subscripts

| | |
|---|---|
| a | refers to air |
| c | refers to spar cap |
| s | refers to the skin |
| 1,2 | the beginning and the end of time interval $\tau$ |

Equations (A1) and (A2) do not take into consideration heat transferred by radiation, since it would be small at these surface temperatures and altitudes; also the heat transferred by convection to the air inside the wing was assumed negligible. The equation used for the determination of the surface heat-transfer coefficient was that given in reference 4 for turbulent flow. The use of a surface heat-transfer coefficient for turbulent flow was based on

the local Reynolds number at the spar-cap location which varied from approximately 1,500,000 to 6,000,000 throughout the dives.

The area of the spar cap $S_c$ used in equation (A1) was the surface area of a 1-foot length of the spar cap. The area of the skin $S_s$ used in equation (A2) was based on a 1-foot length of the skin and on a width which was considered as representative of that portion of the skin which transferred heat to the spar cap, namely, between the spar cap and the adjacent stiffener. The distance for heat flow $l$ between the skin and the spar cap in both equations (A1) and (A2) was taken as the distance between the spar cap and the center of the surface area of the skin. Since the spar cap received heat from the skin on either side, the total heat transferred to the spar cap was assumed twice that transferred from the skin on one side of the spar cap. The temperature of the air $t_a$ in equations (A1) and (A2) is the temperature of the air in the boundary layer. The boundary-layer temperature was considered to be the ambient-air temperature plus the temperature rise as occurs in the boundary layer due to the dissipation of kinetic energy into heat energy. The temperature rise due to the dissipation of kinetic energy was assumed to be 0.9 of the full adiabatic temperature rise.

## REFERENCES

1. Scherrer, Richard: The Effects of Aerodynamic Heating and Heat Transfer on the Surface Temperature of a Body of Revolution in Steady Supersonic Flight. NACA TN No. 1300, 1947.

2. Wood, George P.: Calculation of Surface Temperatures in Steady Supersonic Flight. NACA TN No. 1114, 1946.

3. Jones, Alun R., and Schlaff, Bernard A.: An Investigation of a Thermal Ice-Prevention System for a C-46 Cargo Airplane. VII - Effect of the Thermal System on the Wing-Structure Stresses as Established in Flight. NACA ARR No. 5G20, 1945.

4. Martinelli, R. C., Guibert, A. G., Morrin, E. H., and Boelter, L. M. K.: An Investigation of Aircraft Heaters. VIII - A Simplified Method for the Calculation of the Unit Thermal Conductance Over Wings. NACA, ARR, Mar. 1943.

TABLE I.— WING SURFACE TEMPERATURES AS MEASURED DURING DIVES OF THE AIRPLANE FROM 35,000 FEET TO 5,000 FEET PRESSURE ALTITUDE

FLIGHT 1

| Thermocouples | S1 | | M2 | | M3 | | M4 | | M5 | | M6 | | S7 | | M8 | | S9 | | S10 | | S11 | | M12 | | S13 | |
|---|---|---|---|---|---|---|---|---|---|---|---|---|---|---|---|---|---|---|---|---|---|---|---|---|---|---|
| | Time (min) | Temp. (°F) | Time (min) | Temp. (°F) | Time (min) | Temp. (°F) | Time (min) | Temp. (°F) | Time (min) | Temp. (°F) | Time (min) | Temp. (°F) | Time (min) | Temp. (°F) | Time (min) | Temp. (°F) | Time (min) | Temp. (°F) | Time (min) | Temp. (°F) | Time (min) | Temp. (°F) | Time (min) | Temp. (°F) | Time (min) | Temp. (°F) |
| | 1.03 | -34 | 1.05 | -33 | 1.07 | -29 | 1.06 | -31 | 1.17 | -34 | 1.12 | -37 | 1.88 | -53 | 1.13 | -40 | 1.72 | -46 | 1.73 | -48 | 1.75 | -49 | 1.77 | -53 | 1.78 | -53 |
| | 1.92 | -34 | 1.93 | -34 | 1.95 | -30 | 1.97 | -33 | 2.05 | -35 | 2.0 | -38 | 2.17 | -49 | 2.02 | -40 | 2.13 | -45 | 2.15 | -45 | 2.17 | -45 | 2.18 | -51 | 2.8 | -48 |
| | 2.35 | -31 | 2.37 | -32 | 2.38 | -30 | 2.40 | -32 | 2.48 | -34 | 2.43 | -37 | 2.6 | -30 | 2.45 | -37 | 2.57 | -37 | 2.58 | -39 | 2.6 | -26 | 2.62 | -38 | 2.63 | -26 |
| | 2.78 | -19 | 2.8 | -23 | 2.82 | -29 | 2.83 | -29 | 2.92 | -31 | 2.87 | -31 | 3.03 | 1 | 2.88 | -26 | 2.97 | -21 | 2.98 | -7 | 3.0 | 1 | 3.02 | -13 | 3.03 | 1 |
| | 3.27 | 0 | 3.28 | -7 | 3.30 | -22 | 3.32 | -23 | 3.40 | -25 | 3.35 | -19 | 3.52 | 34 | 3.37 | -1 | 3.37 | -3 | 3.38 | 15 | 3.4 | 26 | 3.42 | 13 | 3.43 | 29 |
| | 3.78 | 23 | 3.80 | 14 | 3.82 | -14 | 3.83 | -11 | 3.92 | -14 | 3.87 | -1 | 4.03 | 56 | 3.88 | 18 | 3.78 | 19 | 3.8 | 37 | 3.82 | 49 | 3.83 | 40 | 3.85 | 53 |
| | 4.27 | 35 | 4.28 | 29 | 4.30 | -1 | 4.32 | 1 | 4.40 | -2 | 4.35 | 15 | 4.52 | 67 | 4.37 | 34 | 4.2 | 35 | 4.22 | 50 | 4.23 | 61 | 4.25 | 59 | 4.27 | 66 |
| | 4.75 | 47 | 4.77 | 41 | 4.78 | 8 | 4.80 | 15 | 4.88 | 9 | 4.83 | 28 | 5.0 | 72 | 4.85 | 45 | 4.65 | 45 | 4.67 | 58 | 4.68 | 67 | 4.7 | 68 | 4.72 | 73 |
| | 5.73 | 61 | 5.75 | 58 | 5.77 | 31 | 5.78 | 37 | 5.87 | 29 | 5.82 | 46 | 5.98 | 81 | 5.83 | 59 | 5.07 | 53 | 5.08 | 63 | 5.10 | 65 | 5.12 | 72 | 5.13 | 75 |
| | 6.75 | 72 | 6.77 | 70 | 6.78 | 49 | 6.80 | 53 | 6.88 | 44 | 6.83 | 58 | 7.0 | 86 | 6.85 | 66 | 5.47 | 58 | 5.48 | 66 | 5.50 | 72 | 5.52 | 73 | 5.53 | 76 |
| | 7.82 | 79 | 7.83 | 76 | 7.85 | 60 | 7.87 | 63 | 7.95 | 56 | 7.9 | 67 | 8.07 | 89 | 7.92 | 75 | 5.88 | 63 | 5.9 | 72 | 5.92 | 76 | 5.93 | 76 | 5.95 | 80 |
| | 8.32 | 82 | 8.33 | 80 | 8.35 | 68 | 8.37 | 70 | 8.65 | 65 | 8.6 | 72 | 8.76 | 90 | 8.62 | 78 | 6.72 | 72 | 6.73 | 77 | 6.75 | 82 | 6.77 | 80 | 6.78 | 85 |
| | -- | -- | -- | -- | -- | -- | -- | -- | -- | -- | -- | -- | -- | -- | -- | -- | 7.53 | 76 | 7.55 | 80 | 7.57 | 84 | 7.58 | 84 | 7.6 | 87 |

FLIGHT 1

| Thermocouples | S14 | | M15 | | M16 | | M17 | | S18 | | M19 | | S20 | | M21 | | A22 | | A23 | | M24 | | M25 | | S26 | |
|---|---|---|---|---|---|---|---|---|---|---|---|---|---|---|---|---|---|---|---|---|---|---|---|---|---|---|
| | Time (min) | Temp. (°F) | Time (min) | Temp. (°F) | Time (min) | Temp. (°F) | Time (min) | Temp. (°F) | Time (min) | Temp. (°F) | Time (min) | Temp. (°F) | Time (min) | Temp. (°F) | Time (min) | Temp. (°F) | Time (min) | Temp. (°F) | Time (min) | Temp. (°F) | Time (min) | Temp. (°F) | Time (min) | Temp. (°F) | Time (min) | Temp. (°F) |
| | 1.80 | -46 | 1.81 | -45 | 1.83 | -43 | 1.85 | -41 | 1.30 | -44 | 1.32 | -45 | 1.37 | -43 | 0.98 | -41 | 1.33 | -36 | 1.35 | -38 | 1.18 | -33 | 1.18 | -38 | 1.8 | -43 |
| | 2.21 | -43 | 2.23 | -43 | 2.25 | -42 | 2.27 | -42 | 2.18 | -39 | 2.20 | -43 | 2.25 | -37 | 1.87 | -40 | 2.22 | -30 | 2.67 | -23 | 2.07 | -33 | 2.08 | -37 | 2.1 | -40 |
| | 2.65 | -38 | 2.67 | -40 | 2.70 | -39 | 2.70 | -41 | 2.62 | -27 | 2.63 | -27 | 2.68 | -9 | 2.30 | -37 | 2.69 | -22 | 3.10 | -9 | 2.5 | -32 | 2.52 | -34 | 2.53 | -27 |
| | 3.05 | -27 | 3.07 | -32 | 3.08 | -31 | 3.10 | -37 | 3.05 | 16 | 3.07 | 3 | 3.12 | 26 | 2.73 | -27 | 3.06 | 1 | 3.58 | 14 | 2.93 | -27 | 2.95 | -28 | 2.97 | 0 |
| | 3.45 | -12 | 3.47 | -19 | 3.48 | -18 | 3.50 | -29 | 3.53 | 50 | 3.55 | 40 | 3.60 | 58 | 3.22 | 14 | 3.97 | 30 | 4.10 | 28 | 3.42 | -19 | 3.43 | -1 | 3.45 | 38 |
| | 3.87 | 6 | 3.88 | -3 | 3.90 | -5 | 3.92 | -19 | 4.05 | 70 | 4.07 | 63 | 4.18 | 73 | 3.73 | 47 | 4.08 | 49 | 4.58 | 41 | 3.93 | -5 | 3.95 | 18 | 3.97 | 56 |
| | 4.30 | 20 | 4.30 | 11 | 4.31 | 7 | 4.33 | -8 | 4.53 | 78 | 4.55 | 74 | 4.60 | 77 | 4.22 | 66 | 4.57 | 62 | 5.07 | 50.5 | 4.42 | 9 | 4.43 | 34 | 4.45 | 65 |
| | 4.73 | 32 | 4.75 | 25 | 4.77 | 19 | 4.78 | 6 | 5.02 | 80 | 5.03 | 79 | 5.08 | 78 | 4.70 | 74 | 5.05 | 68 | 6.05 | 57 | 4.9 | 23 | 4.92 | 45 | 4.93 | 70 |
| | 5.15 | 40 | 5.17 | 35 | 5.18 | 28 | 5.20 | 16 | 6.0 | 85 | 6.02 | 82 | 6.07 | 84 | 5.68 | 79 | 6.03 | 74 | 7.07 | 65 | 5.88 | 43 | 5.90 | 59 | 5.93 | 76 |
| | 5.55 | 47 | 5.57 | 42 | 5.58 | 35 | 5.60 | 24 | 7.02 | 88 | 7.03 | 87 | 7.08 | 88 | 6.7 | 84 | 7.05 | 81 | 8.13 | 70 | 6.90 | 57 | 6.92 | 69 | 6.93 | 83 |
| | 5.97 | 53 | 5.98 | 49 | 6.0 | 43 | 6.02 | 32 | 8.09 | 90 | 8.10 | 89 | 8.15 | 89 | 7.77 | 88 | 8.12 | 84 | 8.83 | 75 | 7.97 | 66 | 7.98 | 74 | 8.0 | 84 |
| | 6.80 | 65 | 6.80 | 60 | 6.83 | 56 | 6.85 | 47 | 8.78 | 89 | 8.80 | 88 | 8.83 | 91 | 8.47 | 85 | 8.82 | 84 | -- | -- | 8.67 | 72 | 8.68 | 78 | 8.7 | 86 |
| | 7.61 | 72 | 7.63 | 69 | 7.65 | 66 | 7.67 | 58 | -- | -- | -- | -- | -- | -- | -- | -- | -- | -- | -- | -- | -- | -- | -- | -- | -- | -- |

FLIGHT 1

| Thermocouples | M27 | | M28 | | S29 | | F31 | | S32 | | M33 | | S34 | | S35 | | S36 | | M37 | | S42 | | M43 | | S44 | |
|---|---|---|---|---|---|---|---|---|---|---|---|---|---|---|---|---|---|---|---|---|---|---|---|---|---|---|
| | Time (min) | Temp. (°F) | Time (min) | Temp. (°F) | Time (min) | Temp. (°F) | Time (min) | Temp. (°F) | Time (min) | Temp. (°F) | Time (min) | Temp. (°F) | Time (min) | Temp. (°F) | Time (min) | Temp. (°F) | Time (min) | Temp. (°F) | Time (min) | Temp. (°F) | Time (min) | Temp. (°F) | Time (min) | Temp. (°F) | Time (min) | Temp. (°F) |
| | 1.23 | -44 | 1.25 | -46 | 1.27 | -46 | 1.56 | -8 | 2.02 | -23 | 2.0 | -17 | 2.03 | -24 | 2.05 | -42 | 2.07 | -42 | 2.08 | -41 | 1.87 | -58 | 1.93 | -56 | 1.92 | -56 |
| | 2.12 | -43 | 2.13 | -44 | 2.15 | -42 | 2.40 | -21 | 2.43 | -17 | 2.42 | -27 | 2.45 | -27 | 2.47 | -24 | 2.48 | -34 | 2.50 | -37 | 2.28 | -47 | 2.37 | -51 | 2.33 | -48 |
| | 2.55 | -38 | 2.57 | -37 | 2.58 | -25 | 2.83 | -25 | 2.87 | 1 | 2.85 | -9 | 2.88 | 1 | 2.50 | 2 | 2.52 | -23 | 2.53 | -21 | 2.72 | -16 | 2.80 | -37 | 2.73 | -9 |
| | 2.98 | -26 | 3.0 | -17 | 3.02 | 1 | 3.23 | -14 | 3.27 | 20 | 3.25 | 5 | 3.28 | 21 | 3.30 | 27 | 3.32 | 9 | 3.33 | -2 | 3.12 | 15 | 3.20 | -14 | 3.17 | 26 |
| | 3.47 | -4 | 3.48 | 10 | 3.50 | 31 | 3.63 | -11 | 3.67 | 38 | 3.69 | 17 | 3.68 | 40 | 3.70 | 50 | 3.72 | 30 | 3.73 | 20 | 3.52 | 41 | 3.60 | 9 | 3.57 | 54 |
| | 3.98 | 18 | 4.0 | 33 | 4.02 | 55 | 4.05 | -8 | 4.08 | 49 | 4.07 | 37 | 4.10 | 50 | 4.12 | 62 | 4.13 | 49 | 4.15 | 41 | 3.93 | 61 | 4.02 | 33 | 3.98 | 73 |
| | 4.47 | 37 | 4.48 | 50 | 4.50 | 65 | 4.47 | -2 | 4.50 | 52 | 4.48 | 32 | 4.52 | 55 | 4.53 | 69 | 4.55 | 59 | 4.57 | 54 | 4.35 | 69 | 4.43 | 50 | 4.40 | 77 |
| | 4.95 | 51 | 4.97 | 61 | 4.98 | 71 | 4.92 | 3 | 4.95 | 53 | 4.93 | 33 | 4.97 | 57 | 4.98 | 71 | 5.0 | 65 | 5.02 | 61 | 4.80 | 74 | 4.88 | 60 | 4.85 | 80 |
| | 5.93 | 65 | 5.95 | 71 | 5.97 | 79 | 5.33 | 6 | 5.37 | 54 | 5.35 | 37 | 5.38 | 57 | 5.40 | 73 | 5.42 | 67 | 5.43 | 65 | 5.22 | 74 | 5.30 | 66 | 5.27 | 78 |
| | 6.95 | 74 | 6.97 | 80 | 6.98 | 86 | 5.73 | 10 | 5.77 | 58 | 5.75 | 41 | 5.78 | 62 | 5.80 | 77 | 5.82 | 71 | 5.83 | 68 | 5.62 | 78 | 5.70 | 69 | 5.67 | 81 |
| | 8.02 | 78 | 8.03 | 82 | 8.05 | 87 | 6.15 | 11 | 6.18 | 62 | 6.17 | 42 | 6.20 | 66 | 6.23 | 82 | 6.25 | 75 | 6.27 | 72 | 6.03 | 82 | 6.12 | 72 | 6.08 | 86 |
| | 8.72 | 81 | 8.73 | 84 | 8.75 | 89 | 6.98 | 13 | 7.02 | 62 | 7.0 | 43 | 7.03 | 67 | 7.05 | 83 | 7.07 | 79 | 7.08 | 78 | 6.87 | 86 | 6.95 | 79 | 6.92 | 87 |
| | -- | -- | -- | -- | -- | -- | 7.80 | 18 | 7.83 | 65 | 7.82 | 48 | 7.85 | 69 | 7.87 | 86 | 7.88 | 82 | 7.90 | 81 | 7.68 | 87 | 7.77 | 82 | 7.75 | 88 |

FLIGHT 2

| Thermocouples | S1 | | M2 | | M3 | | M4 | | M5 | | M6 | | S7 | | M8 | | S9 | | S10 | | S11 | | M12 | |
|---|---|---|---|---|---|---|---|---|---|---|---|---|---|---|---|---|---|---|---|---|---|---|---|---|
| | Time (min) | Temp. (°F) | Time (min) | Temp. (°F) | Time (min) | Temp. (°F) | Time (min) | Temp. (°F) | Time (min) | Temp. (°F) | Time (min) | Temp. (°F) | Time (min) | Temp. (°F) | Time (min) | Temp. (°F) | Time (min) | Temp. (°F) | Time (min) | Temp. (°F) | Time (min) | Temp. (°F) | Time (min) | Temp. (°F) |
| | 0.73 | -37 | 0.77 | -36 | 0.78 | -32 | 0.80 | -34 | 0.86 | -38 | 0.83 | -40 | 1.0 | -52 | 0.85 | -42 | 0.88 | -48 | 0.90 | -50 | 0.92 | -51 | 0.93 | -53 |
| | 1.18 | -36 | 1.20 | -36 | 1.22 | -32 | 1.23 | -35 | 1.32 | -37 | 1.27 | -40 | 1.43 | -42 | 1.26 | -42 | 1.28 | -47 | 1.30 | -47 | 1.32 | -47 | 1.33 | -51 |
| | 1.63 | -30 | 1.65 | -31 | 1.67 | -31 | 1.68 | -33 | 1.77 | -36 | 1.72 | -38 | 1.88 | -26 | 1.73 | -37 | 1.78 | -40 | 1.73 | -36 | 1.75 | -33 | 1.77 | -39 |
| | 2.07 | -25 | 2.08 | -27 | 2.10 | -30 | 2.12 | -30 | 2.20 | -32 | 2.15 | -33 | 2.32 | -14 | 2.17 | -30 | 2.18 | -34 | 2.13 | -28 | 2.15 | -23 | 2.17 | -27 |
| | 2.48 | -17 | 2.50 | -19 | 2.52 | -26 | 2.53 | -26 | 2.62 | -30 | 2.57 | -28 | 2.75 | 0 | 2.56 | -20 | 2.53 | -27 | 2.55 | -20 | 2.57 | -15 | 2.58 | -17 |
| | 2.93 | -8 | 2.95 | -11 | 2.97 | -22 | 2.98 | -22 | 3.07 | -25 | 3.08 | -21 | 3.18 | 18 | 3.03 | -15 | 2.98 | -20 | 2.93 | -11 | 2.95 | -4 | 2.97 | -9 |
| | 3.37 | 7 | 3.38 | 2 | 3.40 | -16 | 3.42 | -14 | 3.50 | -19 | 3.45 | -12 | 3.63 | 32 | 3.47 | -2 | 3.32 | -8 | 3.33 | 3 | 3.35 | 12 | 3.37 | 8 |
| | 3.88 | 21 | 3.90 | 15 | 3.92 | -7 | 3.93 | -5 | 4.02 | -10 | 3.97 | -1 | 4.13 | 46 | 3.98 | 12 | 3.73 | 5 | 3.72 | 16 | 3.73 | 25 | 3.75 | 23 |
| | 4.33 | 33 | 4.35 | 28 | 4.37 | 2 | 4.38 | 5 | 4.47 | -2 | 4.42 | 12 | 4.60 | 58 | 4.43 | 27 | 4.12 | 20 | 4.13 | 32 | 4.15 | 42 | 4.17 | 38 |
| | 4.85 | 41 | 4.87 | 38 | 4.88 | 12 | 4.90 | 16 | 4.98 | 8 | 4.93 | 23 | 5.10 | 63 | 4.95 | 36 | 4.53 | 32 | 4.55 | 42 | 4.57 | 51 | 4.58 | 51 |
| | 5.83 | 52 | 5.85 | 50 | 5.87 | 29 | 5.88 | 33 | 5.97 | 26 | 5.92 | 37 | 6.08 | 67 | 5.93 | 48 | 4.95 | 39 | 4.97 | 48 | 4.98 | 54 | 5.40 | 60 |
| | 6.30 | 56 | 6.32 | 54 | 6.33 | 35 | 6.35 | 40 | 6.43 | 31 | 6.38 | 42 | 6.55 | 69 | 6.40 | 52 | 5.35 | 45 | 5.37 | 51 | 5.38 | 57 | 5.83 | 62 |
| | 7.27 | 60 | 7.28 | 60 | 7.30 | 45 | 7.32 | 49 | 7.40 | 40 | 7.35 | 50 | 7.52 | 69 | 7.37 | 56 | 5.78 | 50 | 5.80 | 55 | 5.82 | 60 | 6.27 | 63 |
| | 8.25 | 63 | 8.27 | 62 | 8.28 | 51 | 8.30 | 54 | 8.38 | 46 | 8.33 | 54 | 8.50 | 68 | 8.35 | 59 | 6.63 | 56 | 6.65 | 60 | 6.67 | 63 | 6.68 | 64 |

NACA

TABLE I.- CONTINUED

FLIGHT 2

| Thermocouples | S13 | | S14 | | M15 | | M16 | | M17 | | S18 | | M19 | | S20 | | M21 | | A22 | | A23 | | M24 | | M25 | |
|---|---|---|---|---|---|---|---|---|---|---|---|---|---|---|---|---|---|---|---|---|---|---|---|---|---|---|
| | Time (min) | Temp. (°F) | Time (min) | Temp. (°F) | Time (min) | Temp. (°F) | Time (min) | Temp. (°F) | Time (min) | Temp. (°F) | Time (min) | Temp. (°F) | Time (min) | Temp. (°F) | Time (min) | Temp. (°F) | Time (min) | Temp. (°F) | Time (min) | Temp. (°F) | Time (min) | Temp. (°F) | Time (min) | Temp. (°F) | Time (min) | Temp. (°F) |
| | 0.95 | -53 | 0.97 | -47 | 0.98 | -45 | 1.0 | -44 | 1.02 | -41 | 1.02 | -44 | 1.03 | -46 | 1.08 | -44 | 0.70 | -42 | 1.05 | -37 | 1.07 | -41 | 0.03 | -35 | 0.05 | -40 |
| | 1.35 | -48 | 1.37 | -45 | 1.38 | -45 | 1.40 | -42 | 1.42 | -41 | 1.45 | -33 | 1.47 | -39 | 1.52 | -29 | 1.13 | -42 | 1.48 | -31 | 1.50 | -38 | 0.90 | -36 | 1.13 | -40 |
| | 1.78 | -32 | 1.80 | -40 | 1.82 | -41 | 1.83 | -40 | 1.85 | -40 | 1.90 | -19 | 1.92 | -25 | 1.97 | -15 | 1.58 | -32 | 1.93 | -19 | 1.95 | -26 | 1.33 | -35 | 1.80 | -15 |
| | 2.18 | -20 | 2.20 | -35 | 2.22 | -37 | 2.23 | -37 | 2.25 | -38 | 2.33 | -6 | 2.35 | -12 | 2.40 | -3 | 2.02 | -18 | 2.37 | -10 | 2.38 | -18 | 1.76 | -34 | 2.23 | -27 |
| | 2.60 | -10 | 2.62 | -29 | 2.63 | -31 | 2.65 | -31 | 2.67 | -34 | 2.77 | 6 | 2.78 | 1 | 2.83 | 10 | 2.43 | -9 | 2.78 | 1 | 2.80 | -10 | 2.22 | -30 | 3.10 | -10 |
| | 2.98 | 2 | 3.0 | -21 | 3.02 | -24 | 3.03 | -24 | 3.05 | -29 | 3.20 | 22 | 3.22 | 16 | 3.27 | 28 | 2.88 | 5 | 3.23 | 12 | 3.25 | 0 | 3.08 | -20 | 4.05 | 16 |
| | 3.38 | 18 | 3.40 | -11 | 3.42 | -15 | 3.43 | -15 | 3.45 | -22 | 3.65 | 39 | 3.67 | 33 | 3.72 | 43 | 3.32 | 21 | 3.67 | 26 | 3.68 | 15 | 4.03 | -2 | 5.02 | 37 |
| | 3.77 | 31 | 3.78 | 0 | 3.80 | -5 | 3.82 | -5 | 3.83 | -14 | 4.15 | 56 | 4.17 | 50 | 4.22 | 60 | 3.83 | 37 | 4.18 | 40 | 4.20 | 27 | 5.0 | 19 | 6.0 | 50 |
| | 4.18 | 48 | 4.20 | 14 | 4.22 | 7 | 4.23 | 6 | 4.25 | -4 | 4.62 | 62 | 4.63 | 60 | 4.68 | 63 | 4.28 | 53 | 4.63 | 51 | 4.65 | 35 | 5.98 | 36 | 6.47 | 58 |
| | 4.60 | 57 | 4.62 | 24 | 4.63 | 18 | 4.65 | 16 | 4.67 | 6 | 5.12 | 65 | 5.13 | 63 | 5.18 | 64 | 4.80 | 62 | 5.15 | 57 | 5.17 | 42 | 6.45 | 41 | 7.43 | 56 |
| | 5.42 | 63 | 5.03 | 32 | 5.05 | 28 | 5.07 | 24 | 5.08 | 15 | 6.10 | 69 | 6.12 | 67 | 6.17 | 67 | 5.78 | 65 | 6.13 | 62 | 6.15 | 51 | 7.41 | 49 | 8.42 | 58 |
| | 5.85 | 65 | 5.43 | 39 | 5.45 | 35 | 5.47 | 32 | 5.48 | 23 | 6.57 | 68 | 6.58 | 68 | 6.63 | 68 | 6.25 | 67 | 6.60 | 63 | 6.62 | 54 | 8.40 | 53 | 9.42 | 60 |
| | 6.28 | 66 | 5.87 | 44 | 5.88 | 42 | 5.90 | 38 | 5.92 | 31 | 7.53 | 68 | 7.55 | 68 | 7.60 | 68 | 7.22 | 67 | 7.57 | 64 | 7.58 | 58 | 9.40 | 56 | -- | -- |
| | 6.70 | 66 | 6.30 | 50 | 6.32 | 46 | 6.33 | 44 | 6.35 | 27 | 8.52 | 67 | 8.53 | 67 | 8.58 | 67 | 8.20 | 68 | 8.55 | 65 | 8.57 | 60 | -- | -- | -- | -- |

FLIGHT 2

| Thermocouples | S26 | | M27 | | M28 | | S29 | | F31 | | S32 | | M33 | | S34 | | S35 | | S36 | | M37 | | S42 | | M43 | |
|---|---|---|---|---|---|---|---|---|---|---|---|---|---|---|---|---|---|---|---|---|---|---|---|---|---|---|
| | Time (min) | Temp. (°F) | Time (min) | Temp. (°F) | Time (min) | Temp. (°F) | Time (min) | Temp. (°F) | Time (min) | Temp. (°F) | Time (min) | Temp. (°F) | Time (min) | Temp. (°F) | Time (min) | Temp. (°F) | Time (min) | Temp. (°F) | Time (min) | Temp. (°F) | Time (min) | Temp. (°F) | Time (min) | Temp. (°F) | Time (min) | Temp. (°F) |
| | 0.07 | -46 | 0.95 | -45 | 0.97 | -48 | 0.98 | -48 | 1.15 | -88 | 1.18 | -34 | 1.17 | -30 | 1.20 | -32 | 1.22 | -38 | 1.23 | -39 | 1.25 | -38 | 1.03 | -53 | 1.18 | -52 |
| | 0.93 | -46 | 1.38 | -45 | 1.40 | -45 | 1.42 | -42 | 1.55 | -31 | 1.58 | -25 | 1.57 | -28 | 1.60 | -24 | 1.62 | -24 | 1.63 | -30 | 1.65 | -33 | 1.43 | -40 | 1.52 | -47 |
| | 1.37 | -39 | 1.83 | -38 | 1.85 | -35 | 1.87 | -28 | 1.98 | -34 | 2.02 | -19 | 2.0 | -24 | 2.03 | -19 | 2.03 | -16 | 2.07 | -22 | 2.08 | -25 | 1.87 | -25 | 1.95 | -36 |
| | 1.82 | -28 | 2.25 | -29 | 2.28 | -25 | 2.30 | -27 | 2.38 | -33 | 2.42 | -13 | 2.40 | -20 | 2.43 | -13 | 2.45 | -7 | 2.47 | -13 | 2.48 | -16 | 2.27 | -13 | 2.35 | -24 |
| | 2.25 | -16 | 2.70 | -20 | 2.72 | -15 | 2.73 | -6 | 2.80 | -32 | 2.83 | -5 | 2.82 | -14 | 2.85 | -4 | 2.87 | 5 | 2.88 | -4 | 2.90 | -8 | 2.68 | -2 | 2.77 | -14 |
| | 3.12 | 10 | 3.13 | -10 | 3.15 | -3 | 3.18 | 10 | 3.18 | -30 | 3.02 | 7 | 3.20 | -8 | 3.23 | 8 | 3.25 | 20 | 3.27 | 8 | 3.28 | 2 | 3.07 | 11 | 3.15 | 4 |
| | 4.07 | 43 | 3.58 | 3 | 3.60 | 13 | 3.62 | 26 | 3.58 | -28 | 3.62 | 17 | 3.60 | 0 | 3.63 | 17 | 3.65 | 31 | 3.67 | 20 | 3.68 | 14 | 3.47 | 28 | 3.55 | 11 |
| | 5.03 | 56 | 4.08 | 17 | 4.10 | 28 | 4.12 | 44 | 3.97 | -25 | 4.0 | 28 | 3.98 | 6 | 4.02 | 31 | 4.03 | 46 | 4.05 | 33 | 4.07 | 26 | 3.85 | 40 | 3.93 | 2° |
| | 6.02 | 61 | 4.55 | 31 | 4.57 | 42 | 4.58 | 53 | 4.38 | -22 | 4.42 | 37 | 4.40 | 15 | 4.45 | 40 | 4.45 | 55 | 4.47 | 45 | 4.48 | 40 | 4.27 | 56 | 4.35 | 42 |
| | 6.48 | 63 | 5.05 | 42 | 5.07 | 50 | 5.08 | 58 | 4.80 | -19 | 4.83 | 39 | 4.82 | 17 | 4.85 | 42 | 4.87 | 59 | 4.88 | 51 | 4.90 | 49 | 4.68 | 61 | 4.77 | 52 |
| | 7.43 | 63 | 6.03 | 53 | 6.05 | 58 | 6.07 | 64 | 5.62 | -9 | 5.65 | 43 | 5.63 | 24 | 5.67 | 47 | 5.68 | 63 | 5.70 | 58 | 5.72 | 56 | 5.10 | 63 | 5.18 | 57 |
| | 8.43 | 64 | 6.50 | 56 | 6.52 | 61 | 6.53 | 65 | 6.05 | -6 | 6.05 | 43 | 6.07 | 26 | 6.10 | 48 | 6.12 | 64 | 6.13 | 60 | 6.15 | 59 | 5.90 | 65 | 5.98 | 60 |
| | 9.43 | 64 | 7.47 | 60 | 7.48 | 62 | 7.50 | 66 | 6.48 | -4 | 6.52 | 46 | 6.5 | 28 | 6.53 | 49 | 6.55 | 65 | 6.57 | 61 | 6.58 | 60 | 5.93 | 67 | 6.02 | 62 |
| | -- | -- | 8.45 | 62 | 8.47 | 64 | 8.48 | 67 | 6.90 | 0 | 6.93 | 47 | 6.92 | 30 | 6.95 | 50 | 6.97 | 65 | 6.98 | 63 | 7.0 | 62 | 6.78 | 69 | 6.87 | 65 |

FLIGHT 2

| Thermocouples | S44 | |
|---|---|---|
| | Time (min) | Temp. (°F) |
| | 1.08 | -54 |
| | 1.48 | -46 |
| | 1.92 | -32 |
| | 2.32 | -21 |
| | 2.73 | -11 |
| | 3.12 | 1 |
| | 3.52 | 20 |
| | 3.90 | 48 |
| | 4.32 | 64 |
| | 4.73 | 65 |
| | 5.15 | 65 |
| | 5.55 | 67 |
| | 5.98 | 68 |
| | 6.83 | 68 |
| | -- | -- |

FLIGHT 3

| S1 | | M2 | | M3 | | M4 | | M5 | | M6 | | S7 | | M8 | | S9 | | S10 | | S11 | |
|---|---|---|---|---|---|---|---|---|---|---|---|---|---|---|---|---|---|---|---|---|---|
| Time (min) | Temp. (°F) | Time (min) | Temp. (°F) | Time (min) | Temp. (°F) | Time (min) | Temp. (°F) | Time (min) | Temp. (°F) | Time (min) | Temp. (°F) | Time (min) | Temp. (°F) | Time (min) | Temp. (°F) | Time (min) | Temp. (°F) | Time (min) | Temp. (°F) | Time (min) | Temp. (°F) |
| 0.82 | -24 | 0.83 | -24 | 0.85 | -23 | 0.87 | -23 | 0.07 | -30 | 0.02 | -30 | 0.18 | -47 | 0.03 | -34 | 0.53 | -37 | 0.55 | -38 | 0.57 | -40 |
| 1.68 | -43 | 1.70 | -23 | 1.72 | -23 | 1.73 | -24 | 0.95 | -30 | 0.90 | -30 | 1.07 | -38 | 0.92 | -33 | 1.35 | -32 | 1.37 | -30 | 1.38 | -30 |
| 2.55 | -20 | 2.57 | -20 | 2.58 | -20 | 2.60 | -21 | 1.82 | -29 | 1.77 | -28 | 1.93 | -25 | 1.78 | -28 | 2.13 | -25 | 2.15 | -22 | 2.17 | -20 |
| 3.45 | -13 | 3.47 | -14 | 3.48 | -17 | 3.50 | -18 | 2.68 | -26 | 2.63 | -22 | 2.80 | -13 | 2.65 | -20 | 2.93 | -22 | 2.95 | -20 | 2.97 | -17 |
| 4.33 | -6 | 4.35 | -8 | 4.37 | -11 | 4.38 | -12 | 3.58 | -22 | 3.53 | -15 | 3.70 | -5 | 3.55 | -13 | 2.93 | -19 | 2.95 | -16 | 2.97 | -14 |
| 5.53 | 12 | 5.55 | 8 | 5.57 | 0 | 5.58 | 0 | 4.47 | -16 | 4.42 | -9 | 4.58 | 12 | 4.43 | -4 | 3.33 | -16 | 3.35 | -14 | 3.37 | -11 |
| 6.02 | 20 | 6.03 | 17 | 6.05 | 4 | 6.07 | 6 | 5.67 | -5 | 5.62 | 6 | 5.78 | 29 | 5.63 | 12 | 3.63 | -13 | 3.75 | -9 | 3.77 | -6 |
| 6.48 | 28 | 6.50 | 24 | 6.52 | 11 | 6.53 | 12 | 6.15 | 0 | 6.10 | 11 | 6.27 | 39 | 6.12 | 20 | 4.13 | -8 | 4.15 | -4 | 4.17 | 0 |
| 7.00 | 39 | 7.02 | 34 | 7.03 | 18 | 7.05 | 20 | 6.62 | 6 | 6.57 | 17 | 6.73 | 49 | 6.58 | 27 | 4.52 | -2 | 4.53 | 3 | 4.55 | 8 |
| 7.58 | 54 | 7.60 | 48 | 7.62 | 25 | 7.63 | 29 | 7.13 | 13 | 7.08 | 25 | 7.27 | 63 | 7.10 | 38 | 4.90 | 3 | 4.92 | 10 | 4.93 | 14 |
| 8.12 | 65 | 8.13 | 60 | 8.15 | 34 | 8.17 | 38 | 7.72 | 22 | 7.67 | 36 | 7.83 | 80 | 7.68 | 50 | 5.70 | 13 | 5.72 | 20 | 5.73 | 25 |
| 8.63 | 74 | 8.65 | 69 | 8.67 | 42 | 8.68 | 48 | 8.25 | 31 | 8.20 | 47 | 8.37 | 89 | 8.22 | 62 | 6.10 | 29 | 6.12 | 28 | 6.13 | 33 |
| 9.13 | 81 | 9.15 | 77 | 9.17 | 51 | 9.18 | 56 | 8.73 | 40 | 8.72 | 55 | 8.88 | 94 | 8.73 | 69 | 6.50 | 35 | 6.52 | 43 | 6.53 | 51 |
| 9.68 | 85 | 9.70 | 82 | 9.72 | 59 | 9.73 | 63 | 9.27 | 48 | 9.22 | 64 | 9.38 | 98 | 9.23 | 77 | 7.73 | 56 | 7.75 | 68 | 7.77 | 76 |
| -- | -- | -- | -- | -- | -- | -- | -- | -- | -- | 9.82 | 57 | 9.77 | 70 | -- | -- | -- | -- | 9.00 | 77 | 9.02 | 85 | 9.03 | 91 |

TABLE I.- CONCLUDED

FLIGHT 3

| Thermocouples | M12, | | S13 | | S14 | | M15 | | M16 | | M17 | | S18 | | M19 | | S20 | | M21 | | A22 | | A23 | | M24 | |
|---|---|---|---|---|---|---|---|---|---|---|---|---|---|---|---|---|---|---|---|---|---|---|---|---|---|---|
| | Time (min) | Temp. (°F) | Time (min) | Temp. (°F) | Time (min) | Temp. (°F) | Time (min) | Temp. (°F) | Time (min) | Temp. (°F) | Time (min) | Temp. (°F) | Time (min) | Temp. (°F) | Time (min) | Temp. (°F) | Time (min) | Temp. (°F) | Time (min) | Temp. (°F) | Time (min) | Temp. (°F) | Time (min) | Temp. (°F) | Time (min) | Temp. (°F) |
| | 0.63 | -42 | 0.65 | -43 | 0.67 | -37 | 0.68 | -36 | 0.7 | -33 | 0.72 | -32 | 0.90 | -28 | 0.92 | -30 | 0.97 | -28 | 0.77 | -28 | 0.93 | -20 | 0.85 | -24 | 0.08 | -29 |
| | 1.45 | -34 | 1.47 | -30 | 1.48 | -33 | 1.50 | -33 | 1.52 | -32 | 1.53 | -32 | 1.06 | -27 | 1.10 | -29 | 1.15 | -27 | 1.63 | -23 | 1.12 | -19 | 1.13 | -20 | 0.97 | -29 |
| | 2.23 | -23 | 2.25 | -20 | 2.27 | -28 | 2.28 | -30 | 2.30 | -30 | 2.32 | -31 | 1.55 | -20 | 1.57 | -23 | 2.02 | -20 | 2.50 | -15 | 1.58 | -17 | 2.0 | -17 | 1.83 | -28 |
| | 2.63 | -18 | 2.65 | -16 | 2.67 | -26 | 2.68 | -28 | 2.70 | -27 | 2.72 | -29 | 2.82 | -11 | 2.85 | -14 | 2.88 | -11 | 3.40 | -7 | 2.85 | -10 | 2.87 | -10 | 2.70 | -23 |
| | 3.03 | -15 | 3.05 | -12 | 3.07 | -24 | 3.08 | -25 | 3.10 | -25 | 3.12 | -28 | 3.72 | -3 | 3.73 | -5 | 3.76 | -2 | 4.28 | 4 | 3.75 | -3 | 3.77 | -5 | 3.60 | -18 |
| | 3.43 | -11 | 3.45 | -9 | 3.47 | -22 | 3.48 | -23 | 3.50 | -23 | 3.52 | -25 | 4.60 | 13 | 4.62 | 9 | 4.67 | 14 | 5.48 | 25 | 4.63 | 8 | 4.65 | 4 | 4.48 | -11 |
| | 3.83 | -8 | 3.85 | -4 | 3.87 | -18 | 3.88 | -20 | 3.90 | -20 | 3.92 | -24 | 5.80 | 35 | 5.82 | 31 | 5.87 | 35 | 5.97 | 32 | 5.83 | 26 | 5.85 | 20 | 5.68 | 2 |
| | 4.23 | -1 | 4.25 | 3 | 4.27 | -14 | 4.28 | -16 | 4.30 | -17 | 4.32 | -20 | 6.29 | 43 | 6.30 | 40 | 6.35 | 45 | 6.43 | 41 | 6.32 | 33 | 6.33 | 27 | 6.17 | 9 |
| | 4.62 | 6 | 4.63 | 11 | 4.65 | -9 | 4.67 | -12 | 4.68 | -13 | 4.70 | -17 | 6.75 | 54 | 6.77 | 51 | 6.82 | 57 | 6.93 | 53 | 6.78 | 43 | 6.80 | 36 | 6.63 | 15 |
| | 5.0 | 14 | 5.02 | 18 | 5.03 | -4 | 5.05 | -7 | 5.07 | -8 | 5.08 | -13 | 7.28 | 70 | 7.30 | 65 | 7.35 | 74 | 7.53 | 69 | 7.30 | 55 | 7.32 | 45 | 7.15 | 23 |
| | 5.40 | 19 | 5.42 | 23 | 5.43 | 1 | 5.45 | -2 | 5.47 | -3 | 5.48 | -9 | 7.85 | 88 | 7.87 | 82 | 7.92 | 90 | 8.07 | 84 | 7.88 | 71 | 7.90 | 55 | 7.73 | 32 |
| | 5.80 | 25 | 5.82 | 29 | 5.83 | 7 | 5.85 | 3 | 5.87 | 3 | 5.88 | -5 | 8.39 | 94 | 8.30 | 92 | 8.45 | 94 | 8.58 | 91 | 8.42 | 80 | 8.43 | 63 | 8.27 | 42 |
| | 6.20 | 31 | 6.22 | 37 | 6.23 | 13 | 6.25 | 10 | 6.27 | 8 | 6.28 | 0 | 8.90 | 98 | 8.92 | 96 | 8.97 | 98 | 9.08 | 94 | 8.93 | 86 | 8.95 | 70 | 8.78 | 52 |
| | 7.0 | 48 | 7.02 | 55 | 7.03 | 28 | 7.05 | 24 | 7.07 | 22 | 7.08 | 11 | 9.60 | 100 | 9.42 | 99 | 9.47 | 100 | 9.63 | 97 | 9.43 | 90 | 9.45 | 78 | 9.28 | 59 |
| | 7.83 | 73 | 7.85 | 82 | 7.87 | 49 | 7.88 | 42 | 7.90 | 37 | 7.92 | 26 | -- | -- | -- | -- | -- | -- | -- | -- | -- | -- | -- | -- | 9.63 | 66 |
| | 9.10 | 93 | 9.12 | 97 | 9.13 | 71 | 9.15 | 67 | 9.17 | 63 | 9.18 | 52 | -- | -- | -- | -- | -- | -- | -- | -- | -- | -- | -- | -- | -- | -- |

FLIGHT 3

| Thermocouples | M25 | | S26 | | M27 | | M28 | | S29 | | F31 | | S32 | | M33 | | S34 | | S35 | | S36 | | M37 | | S42 | |
|---|---|---|---|---|---|---|---|---|---|---|---|---|---|---|---|---|---|---|---|---|---|---|---|---|---|---|
| | Time (min) | Temp. (°F) | Time (min) | Temp. (°F) | Time (min) | Temp. (°F) | Time (min) | Temp. (°F) | Time (min) | Temp. (°F) | Time (min) | Temp. (°F) | Time (min) | Temp. (°F) | Time (min) | Temp. (°F) | Time (min) | Temp. (°F) | Time (min) | Temp. (°F) | Time (min) | Temp. (°F) | Time (min) | Temp. (°F) | Time (min) | Temp. (°F) |
| | 0.10 | -34 | 0.12 | -39 | 0.13 | -37 | 0.15 | -38 | 0.17 | -39 | 0.01 | 0 | 0.03 | -11 | 0.03 | -6 | 0.07 | -11 | 0.08 | -33 | 0.10 | -31 | 0.12 | -29 | 0.73 | -47 |
| | 0.98 | -33 | 1.0 | -39 | 1.02 | -39 | 1.03 | -37 | 1.05 | -35 | 0.85 | -1 | 0.88 | -13 | 0.87 | -8 | 0.90 | -13 | 0.92 | -33 | 0.93 | -31 | 0.95 | -30 | 1.55 | -30 |
| | 1.85 | -28 | 1.87 | -24 | 1.88 | -29 | 1.90 | -29 | 1.92 | -24 | 1.67 | -7 | 1.70 | -14 | 1.68 | -11 | 1.72 | -13 | 1.73 | -24 | 1.75 | -25 | 1.76 | -25 | 2.33 | -18 |
| | 2.72 | -20 | 2.73 | -15 | 2.75 | -20 | 2.77 | -19 | 2.78 | -14 | 2.45 | -9 | 2.48 | -11 | 2.47 | -10 | 2.50 | -11 | 2.52 | -16 | 2.53 | -18 | 2.55 | -19 | 2.73 | -14 |
| | 3.62 | -13 | 3.63 | -7 | 3.65 | -12 | 3.67 | -11 | 3.68 | -7 | 2.85 | -10 | 2.88 | -9 | 2.87 | -10 | 2.90 | -9 | 2.92 | -13 | 2.93 | -15 | 2.95 | -16 | 3.13 | -9 |
| | 4.50 | -3 | 4.52 | 8 | 4.53 | -2 | 4.55 | 1 | 4.57 | 9 | 3.25 | -10 | 3.28 | -7 | 3.27 | -8 | 3.30 | -8 | 3.32 | -9 | 3.33 | -12 | 3.35 | -13 | 3.53 | -7 |
| | 5.70 | 14 | 5.72 | 27 | 5.73 | 16 | 5.75 | 19 | 5.77 | 26 | 3.65 | -10 | 3.68 | -5 | 3.67 | -7 | 3.70 | -5 | 3.72 | -5 | 3.73 | -9 | 3.75 | -10 | 3.93 | 0 |
| | 6.18 | 20 | 6.20 | 36 | 6.22 | 22 | 6.23 | 28 | 6.25 | 36 | 4.05 | -8 | 4.08 | 0 | 4.07 | -3 | 4.10 | 0 | 4.12 | 1 | 4.13 | -3 | 4.15 | -5 | 4.33 | 6 |
| | 6.65 | 30 | 6.67 | 46 | 6.68 | 31 | 6.70 | 37 | 6.72 | 48 | 4.45 | -8 | 4.48 | 4 | 4.47 | 0 | 4.50 | 4 | 4.52 | 8 | 4.53 | 2 | 4.55 | 0 | 4.72 | 15 |
| | 7.17 | 39 | 7.18 | 61 | 7.22 | 41 | 7.23 | 50 | 7.25 | 61 | 4.83 | -7 | 4.86 | 11 | 4.85 | 3 | 4.88 | 11 | 4.90 | 15 | 4.92 | 9 | 4.93 | 6 | 5.10 | 31 |
| | 7.75 | 52 | 7.78 | 78 | 7.78 | 54 | 7.80 | 64 | 7.82 | 78 | 5.22 | -9 | 5.25 | 15 | 5.23 | 7 | 5.27 | 16 | 5.28 | 22 | 5.30 | 16 | 5.32 | 13 | 5.50 | 38 |
| | 8.28 | 63 | 8.30 | 85 | 8.32 | 65 | 8.33 | 74 | 8.35 | 86 | 5.62 | -3 | 5.65 | 20 | 5.63 | 11 | 5.67 | 21 | 5.68 | 28 | 5.70 | 22 | 5.72 | 20 | 5.90 | 33 |
| | 8.80 | 70 | 8.82 | 90 | 8.83 | 73 | 8.85 | 82 | 8.87 | 92 | 6.02 | -2 | 6.05 | 26 | 6.03 | 15 | 6.07 | 26 | 6.08 | 36 | 6.10 | 28 | 6.12 | 26 | 6.30 | 40 |
| | 9.30 | 76 | 9.32 | 93 | 9.33 | 80 | 9.35 | 87 | 9.37 | 94 | 6.42 | 0 | 6.45 | 31 | 6.43 | 19 | 6.47 | 33 | 6.48 | 43 | 6.50 | 35 | 6.52 | 32 | 6.70 | 49 |
| | 9.55 | 80 | 9.87 | 95 | -- | -- | -- | -- | -- | -- | 7.22 | 3 | 7.25 | 50 | 7.83 | 30 | 7.27 | 51 | 7.28 | 65 | 7.30 | 53 | 7.32 | 49 | 7.10 | 60 |
| | -- | -- | -- | -- | -- | -- | -- | -- | -- | -- | 8.05 | 12 | 8.08 | 67 | 8.07 | 45 | 8.10 | 70 | 8.12 | 86 | 8.13 | 77 | 8.15 | 78 | 7.93 | 85 |
| | -- | -- | -- | -- | -- | -- | -- | -- | -- | -- | 9.32 | 21 | 9.35 | 76 | 9.33 | 55 | 9.37 | 80 | 9.38 | 98 | 9.40 | 92 | 9.42 | 89 | 9.20 | 99 |

FLIGHT 3

| Thermocouples | S43 | | S44 |
|---|---|---|---|
| | Time (min) | Temp. (°F) | Time (min) | Temp. (°F) |
| | 0.82 | -44 | 0.78 | -43 |
| | 1.63 | -30 | 1.60 | -25 |
| | 2.42 | -19 | 2.38 | -13 |
| | 2.82 | -14 | 2.78 | -10 |
| | 3.22 | -10 | 3.18 | -7 |
| | 3.62 | -7 | 3.58 | -3 |
| | 4.02 | -3 | 3.98 | 3 |
| | 4.42 | 3 | 4.38 | 11 |
| | 4.80 | 10 | 4.77 | 20 |
| | 5.18 | 15 | 5.15 | 23 |
| | 5.58 | 19 | 5.55 | 27 |
| | 5.98 | 24 | 5.95 | 33 |
| | 6.38 | 30 | 6.35 | 42 |
| | 6.78 | 37 | 6.75 | 51 |
| | 7.18 | 46 | 7.15 | 63 |
| | 8.02 | 69 | 7.98 | 88 |
| | 9.28 | 90 | 9.25 | 100 |

FLIGHT 4

| F30 | | F31 | | S32 | | M33 | | S34 | |
|---|---|---|---|---|---|---|---|---|---|
| Time (min) | Temp. (°F) | Time (min) | Temp. (°F) | Time (min) | Temp. (°F) | Time (min) | Temp. (°F) | Time (min) | Temp. (°F) |
| 0.53 | 28 | 0.80 | 11 | 0.83 | -1 | 0.82 | 3 | 0.85 | -1 |
| 1.38 | 26 | 1.58 | 9 | 1.62 | 7 | 1.60 | 6 | 1.63 | 5 |
| 1.72 | 25 | 1.98 | 6 | 2.02 | 10 | 2.0 | 7 | 2.03 | 9 |
| 2.10 | 24 | 2.37 | 6 | 2.40 | 16 | 2.38 | 10 | 2.42 | 14 |
| 2.50 | 24 | 2.77 | 6 | 2.80 | 21 | 2.78 | 15 | 2.82 | 20 |
| 2.88 | 22 | 3.15 | 8 | 3.18 | 28 | 3.17 | 19 | 3.20 | 27 |
| 3.28 | 22 | 3.55 | 10 | 3.58 | 36 | 3.57 | 23 | 3.60 | 37 |
| 3.67 | 22 | 3.93 | 12 | 3.97 | 46 | 3.95 | 30 | 3.98 | 47 |
| 4.08 | 20 | 4.35 | 18 | 4.38 | 60 | 4.37 | 40 | 4.40 | 62 |
| 4.47 | 20 | 4.73 | 22 | 4.77 | 70 | 4.75 | 49 | 4.78 | 72 |
| 4.88 | 23 | 5.15 | 23 | 5.18 | 72 | 5.17 | 52 | 5.20 | 74 |
| 5.30 | 27 | 5.57 | 25 | 5.60 | 74 | 5.58 | 55 | 5.62 | 77 |
| 5.72 | 30 | 5.98 | 27 | 6.02 | 77 | 6.0 | 57 | 6.03 | 80 |
| 6.53 | 37 | 6.80 | 30 | 6.83 | 77 | 6.82 | 58 | 6.85 | 82 |
| 7.35 | 42 | 7.62 | 33 | 7.65 | 79 | 7.63 | 60 | 7.67 | 83 |
| 8.18 | 37 | 8.45 | 38 | 8.48 | 79 | 8.47 | 58 | 8.50 | 84 |
| 9.03 | 44 | 9.60 | 41 | 9.63 | 83 | 9.62 | 67 | 9.65 | 86 |


Figure 1.- High-speed fighter airplane used for thermal stress dive tests.

*Figure 2.- Structural details of right wing of test airplane.*

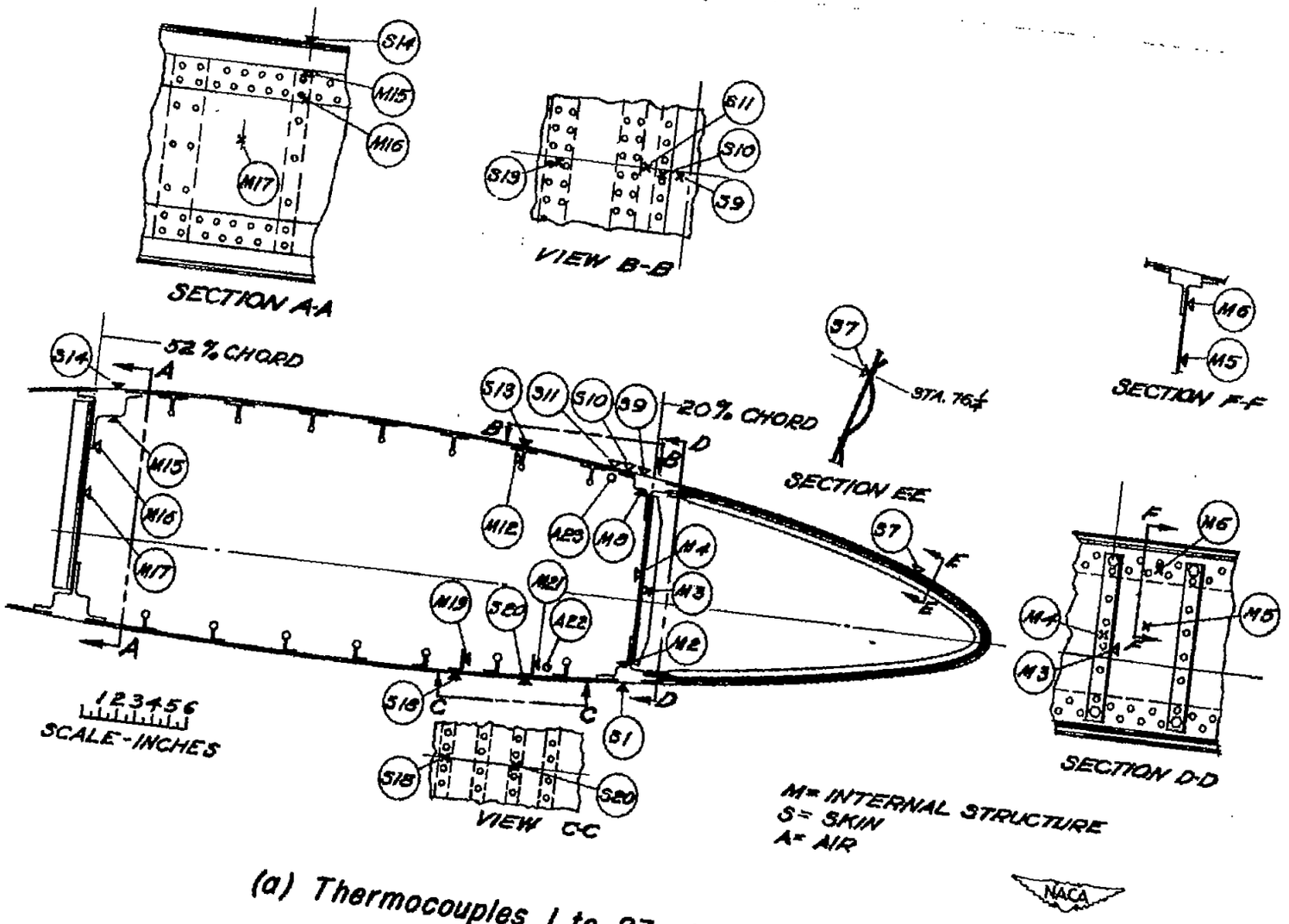


(a) Thermocouples 1 to 23 at station 76 in right wing.

Figure 3.- Thermocouple locations in the wing.

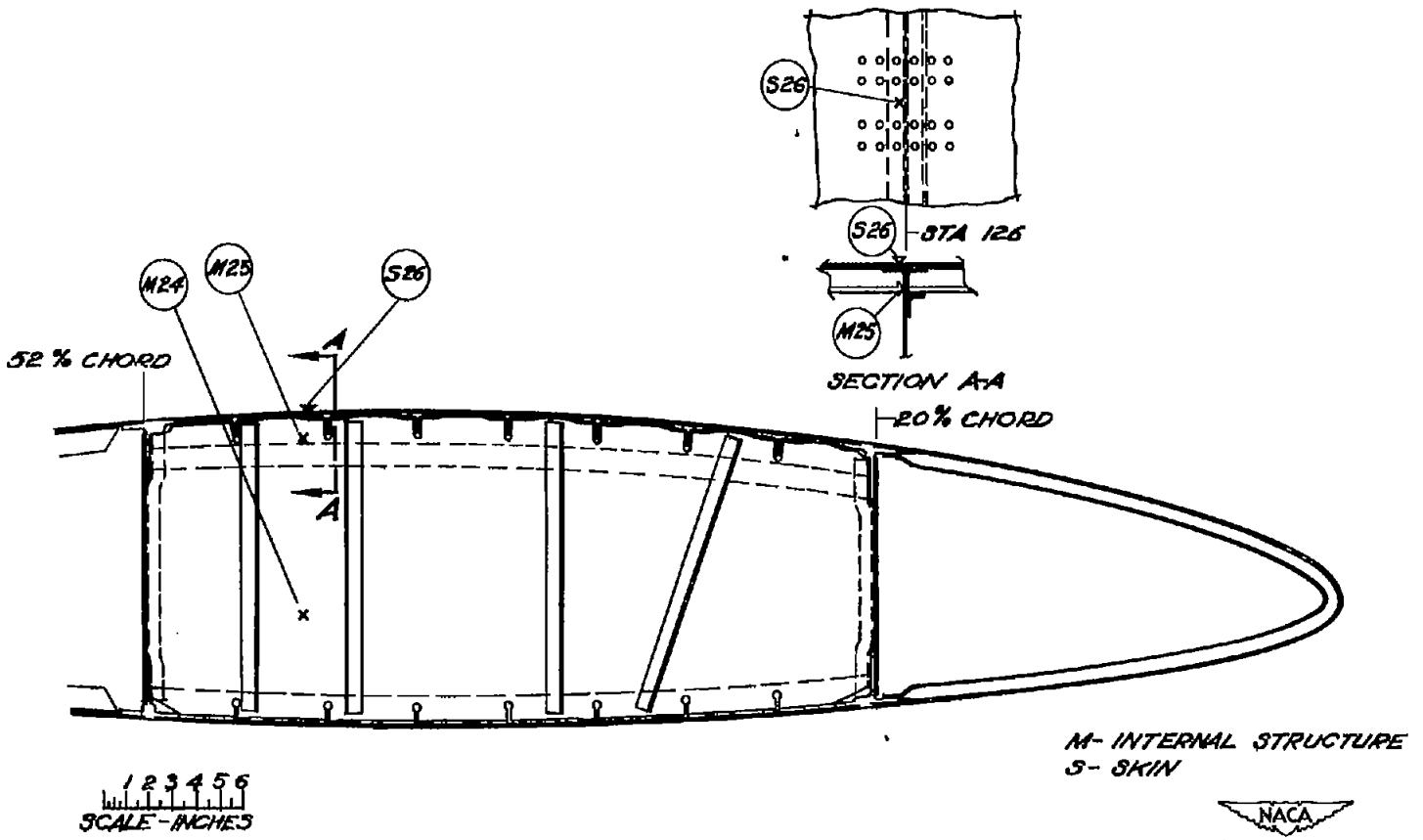


(b) Thermocouples 24 to 26 at station 126 in right wing.

Figure 3.- Continued.

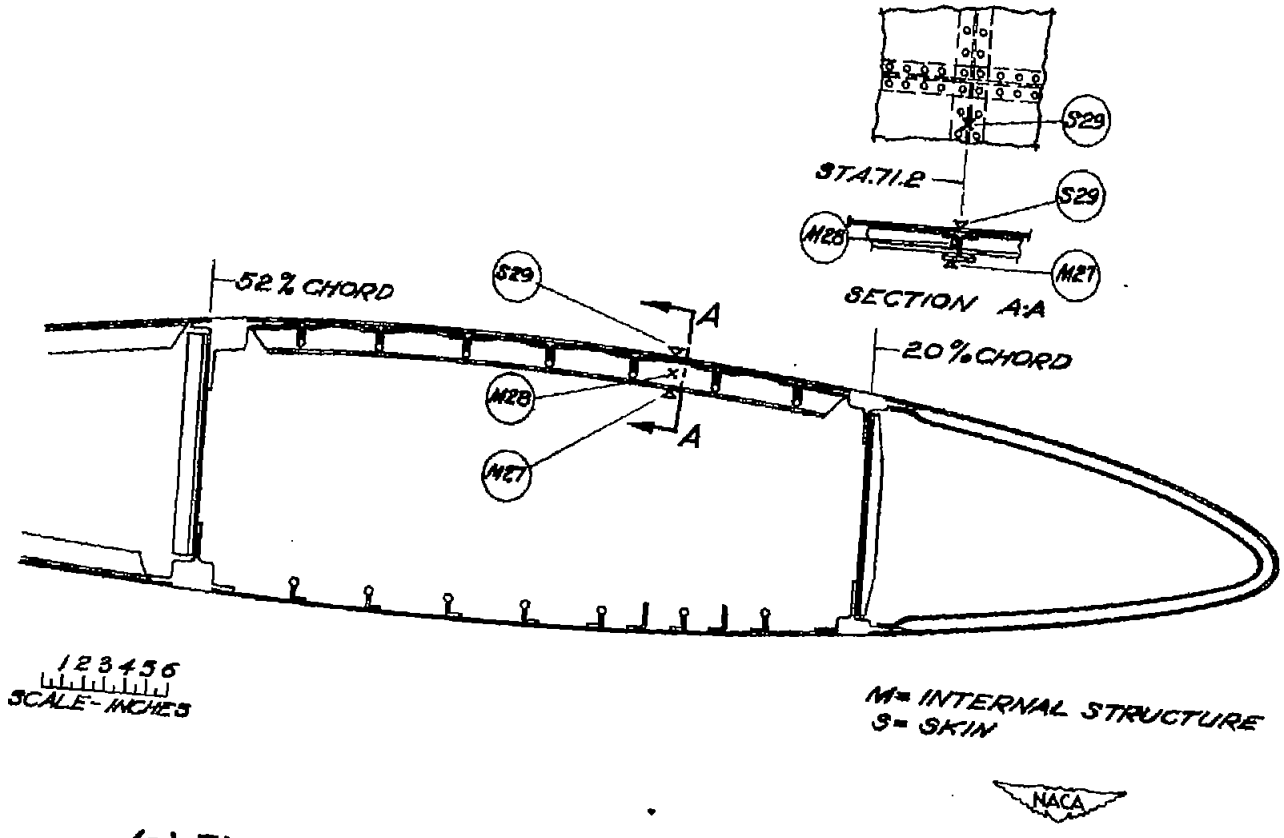


(c) Thermocouples 27 to 29 at station 71.2 in right wing.

Figure 3.- Continued.

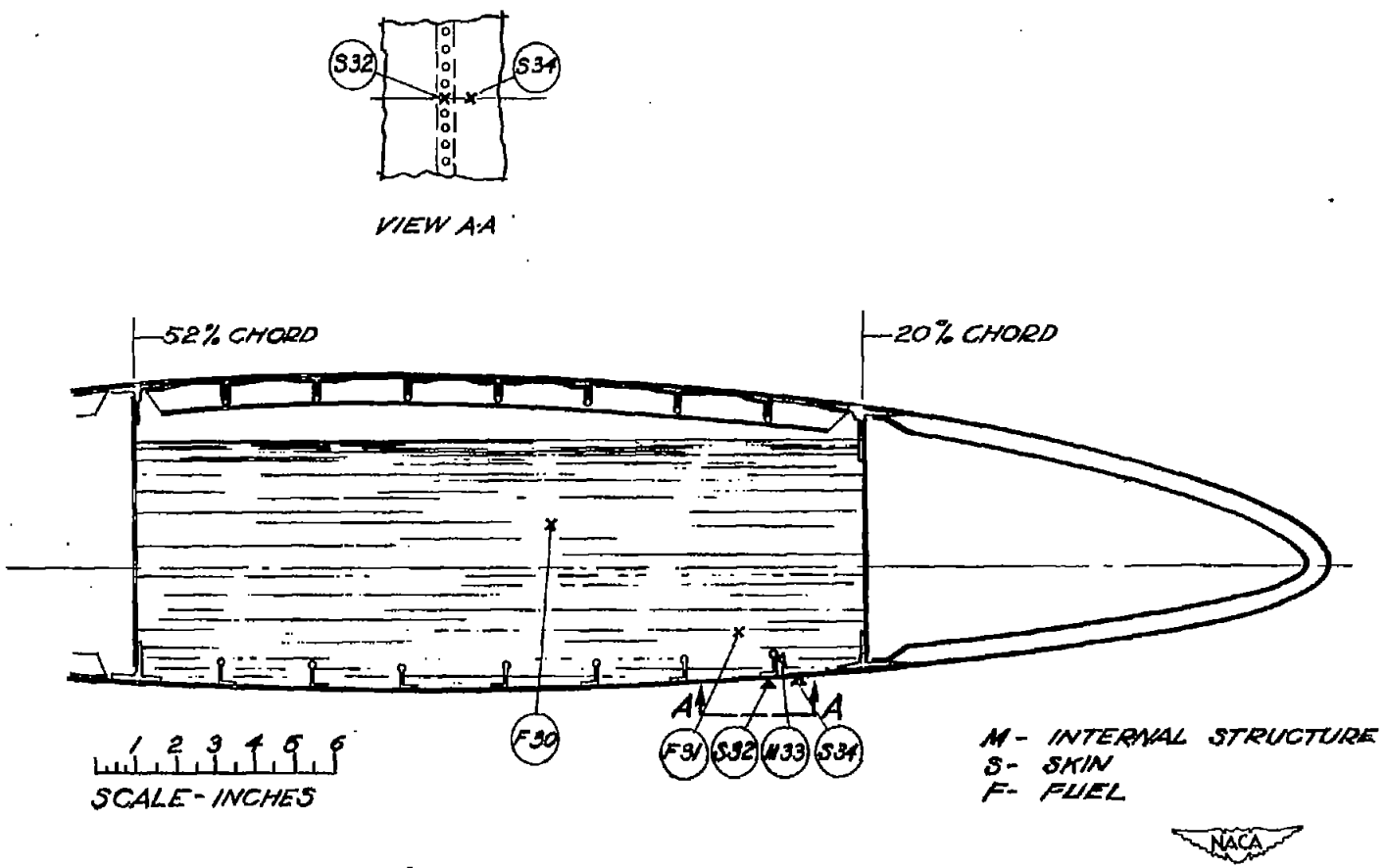


(d) Thermocouples 30 to 34 at integral fuel tank station 153 in right wing.

Figure 3.- Continued.

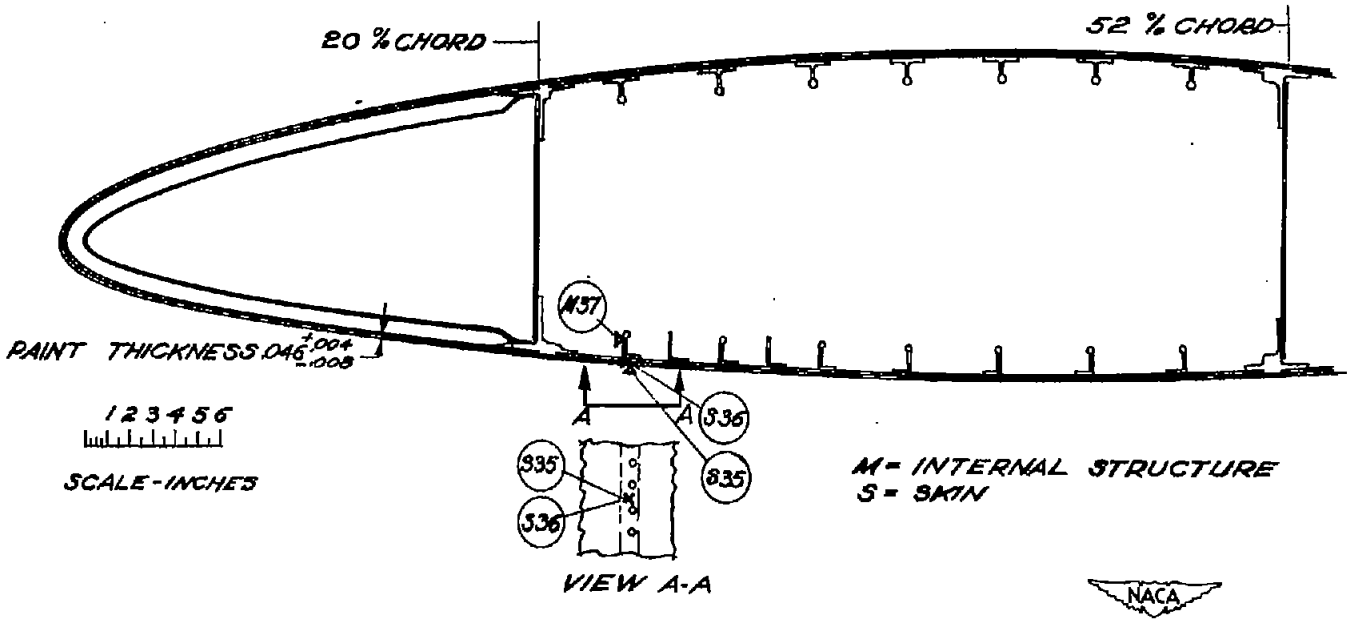


*(e) Thermocouples 35 to 37 at station 112 in left wing.*

*Figure 3.- Continued.*

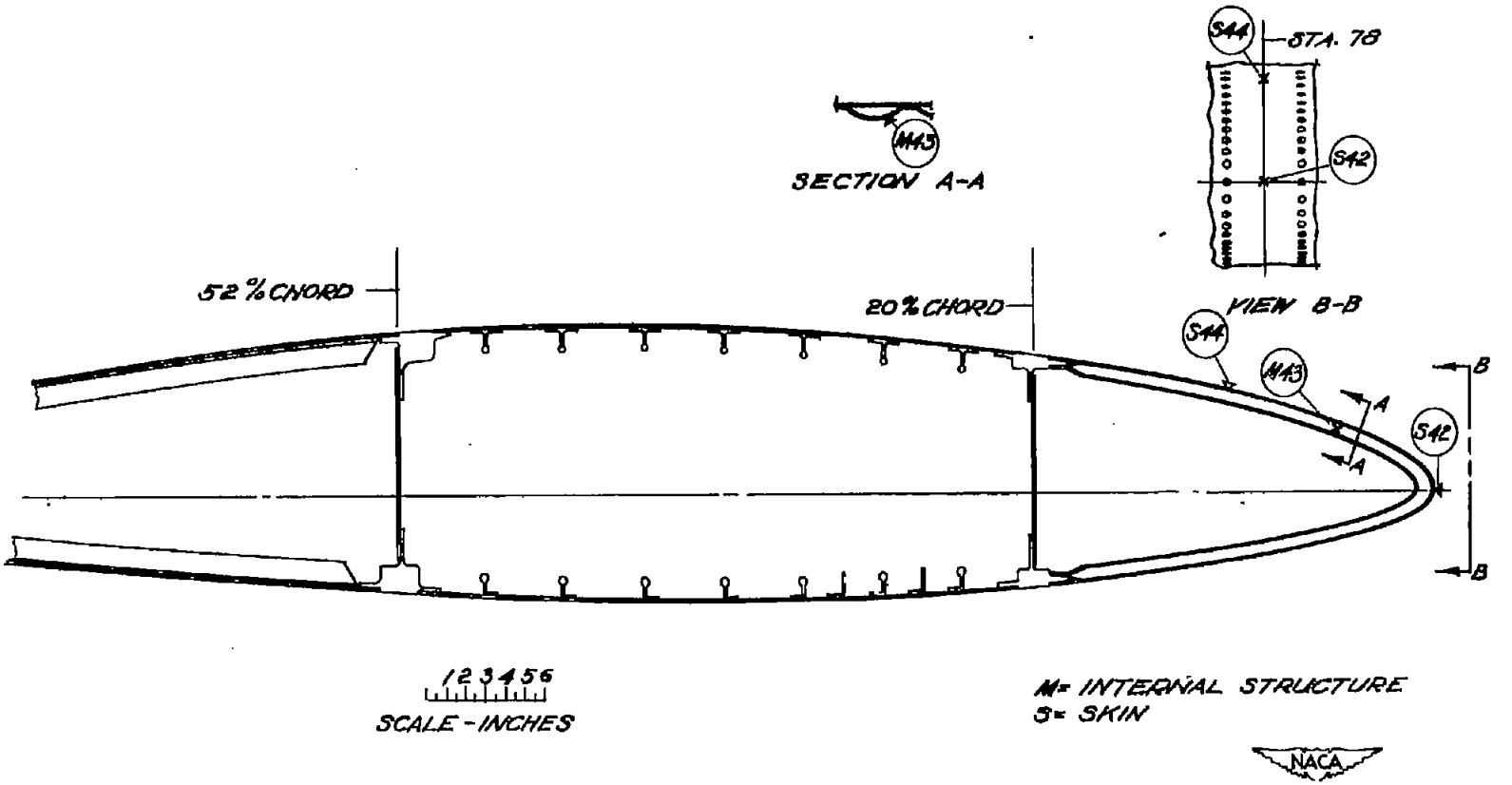


*(f) Thermocouples 42 to 44 at station 77.4 in right wing.*

*Figure 3. Concluded.*

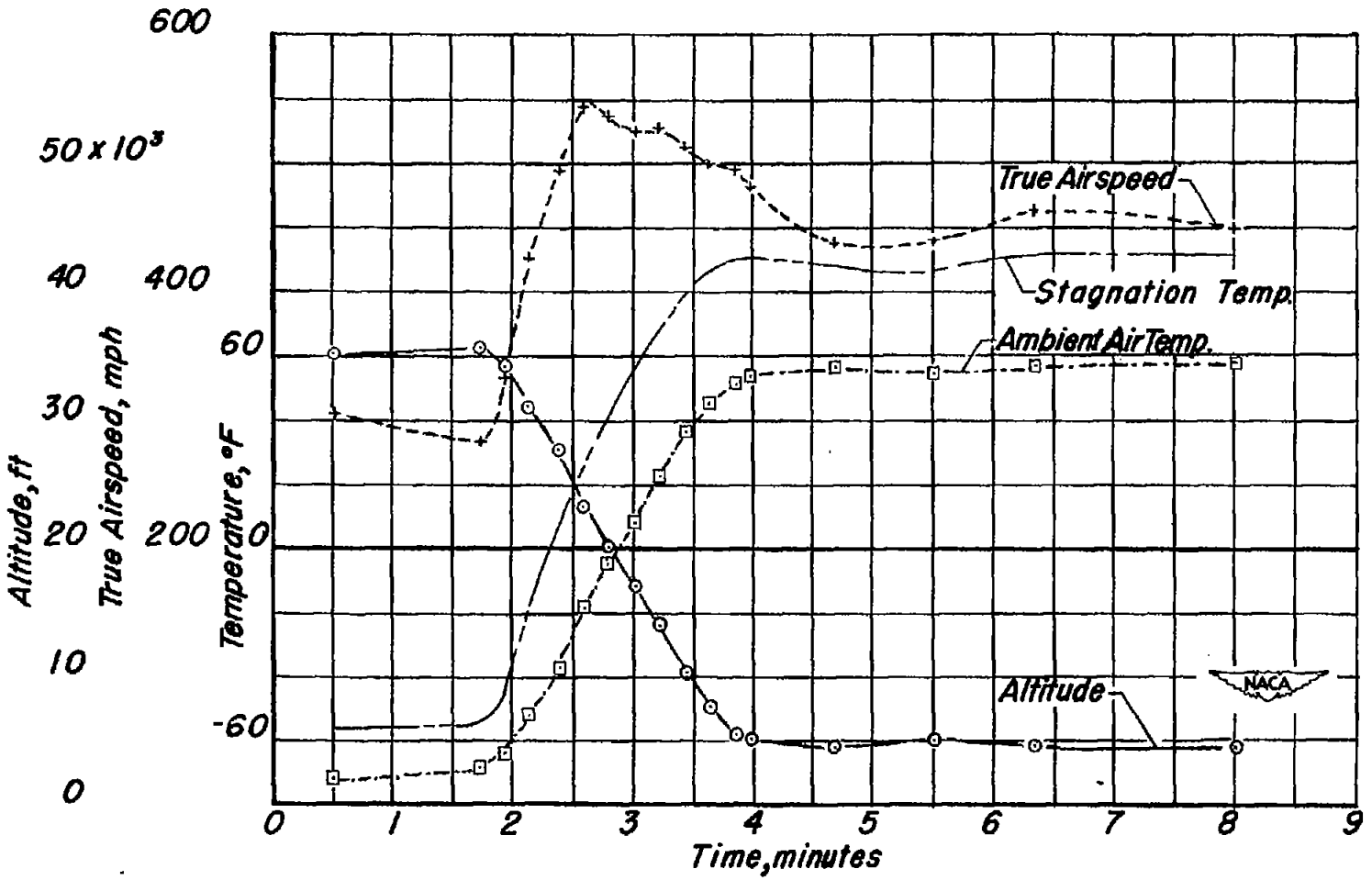


(a) Flight I, average rate of vertical descent 225 ft/sec

Figure 4.- Time histories of airspeed, altitude and ambient-air temperature during the dives from 35,000 feet to 5,000 feet pressure altitude.

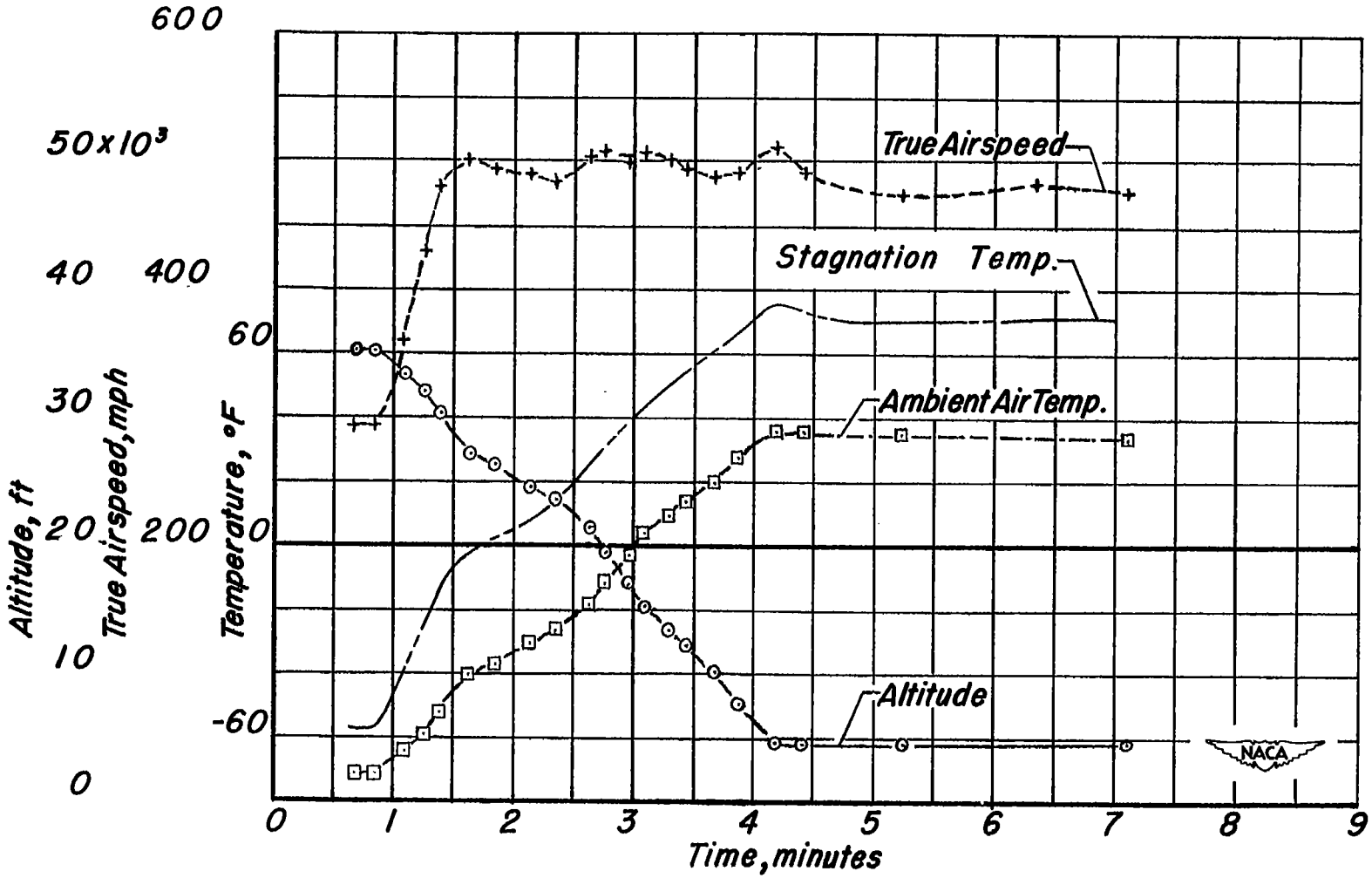


*(b) Flight 2, average rate of vertical descent 150 ft/sec*

*Figure 4.- Continued.*

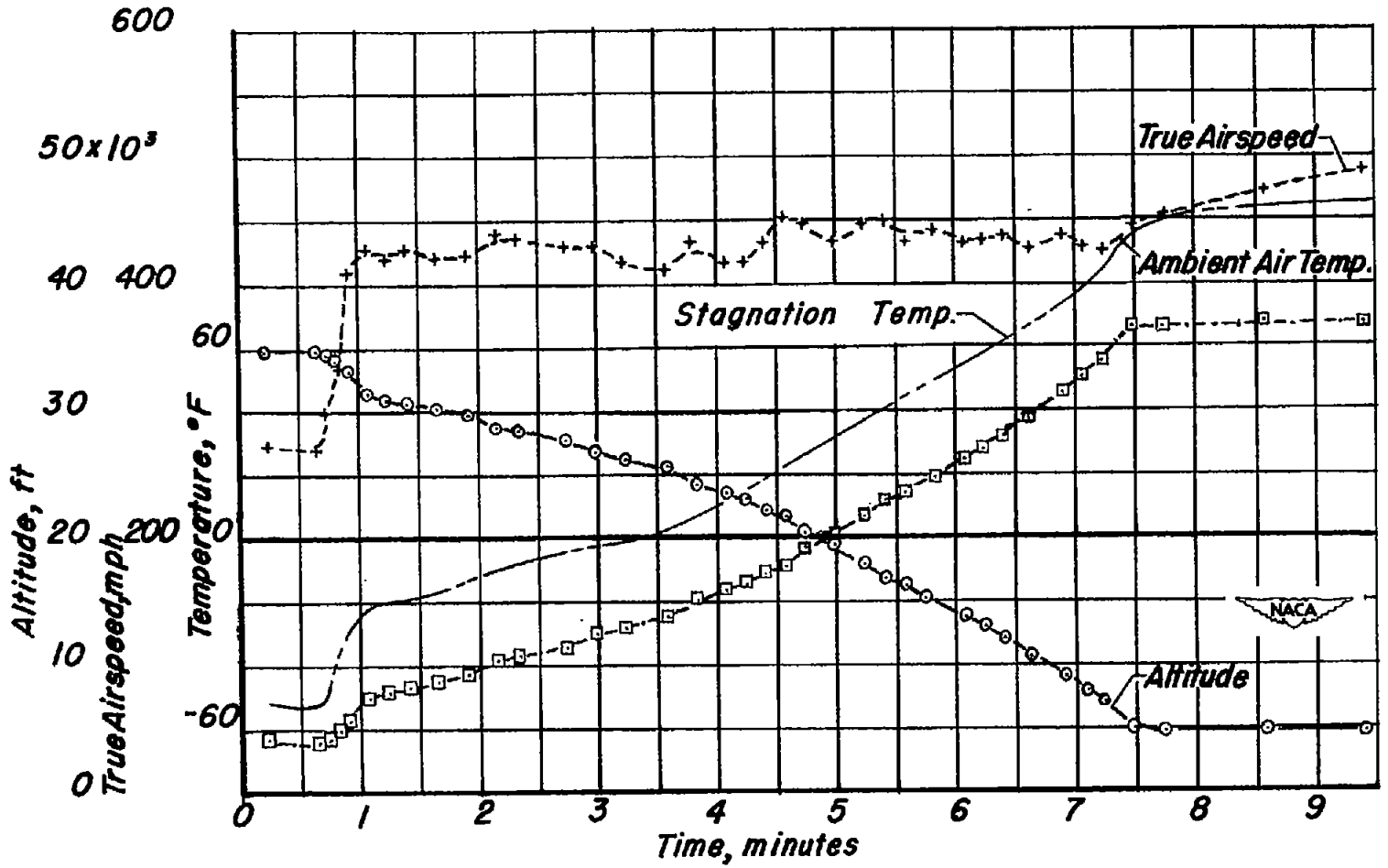


(c) Flight 3, average rate of vertical descent 73 ft/sec

Figure 4.- Continued.

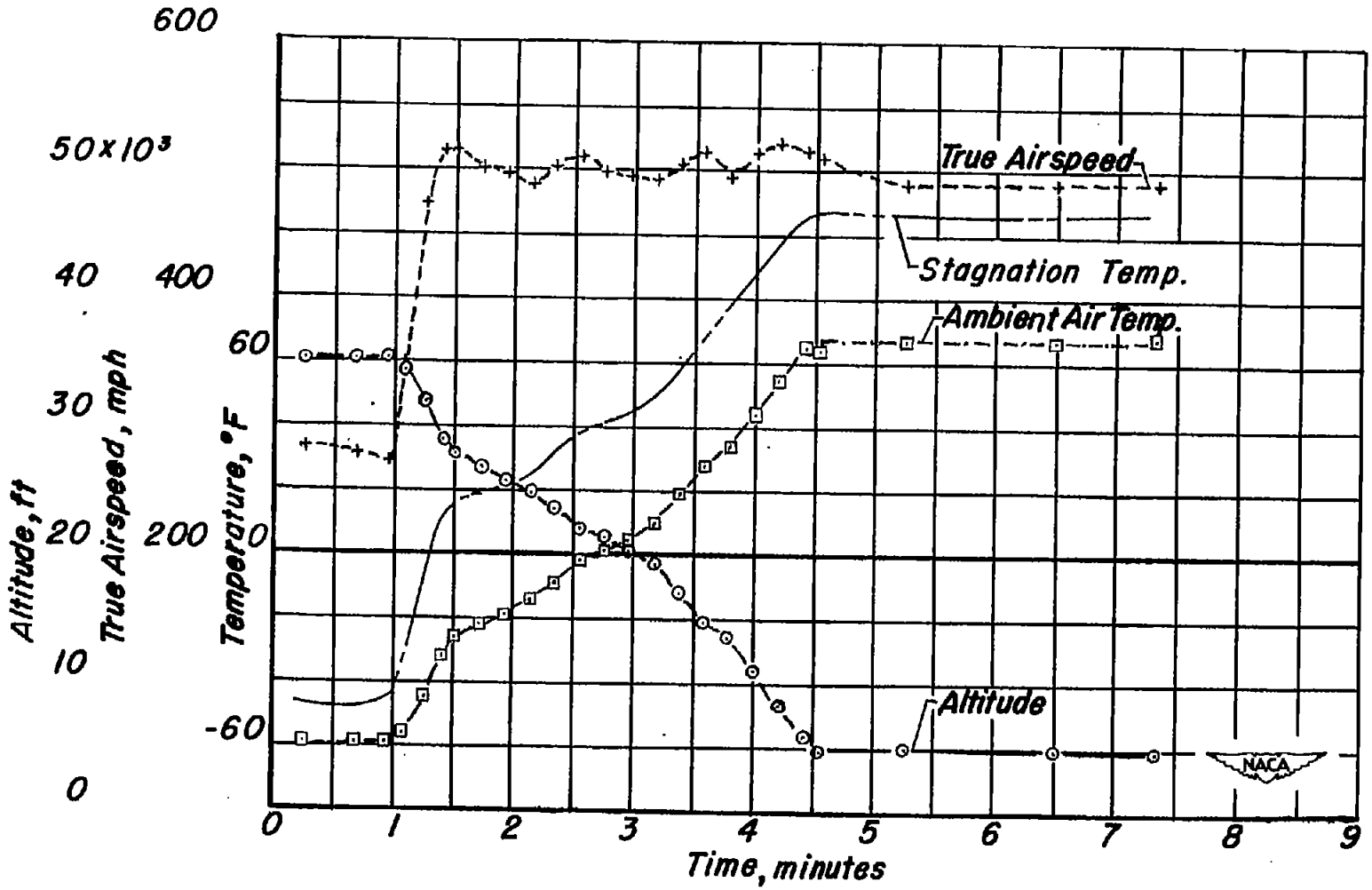


*(d) Flight 4, average rate of vertical descent 138 ft/sec*

*Figure 4.- Concluded.*

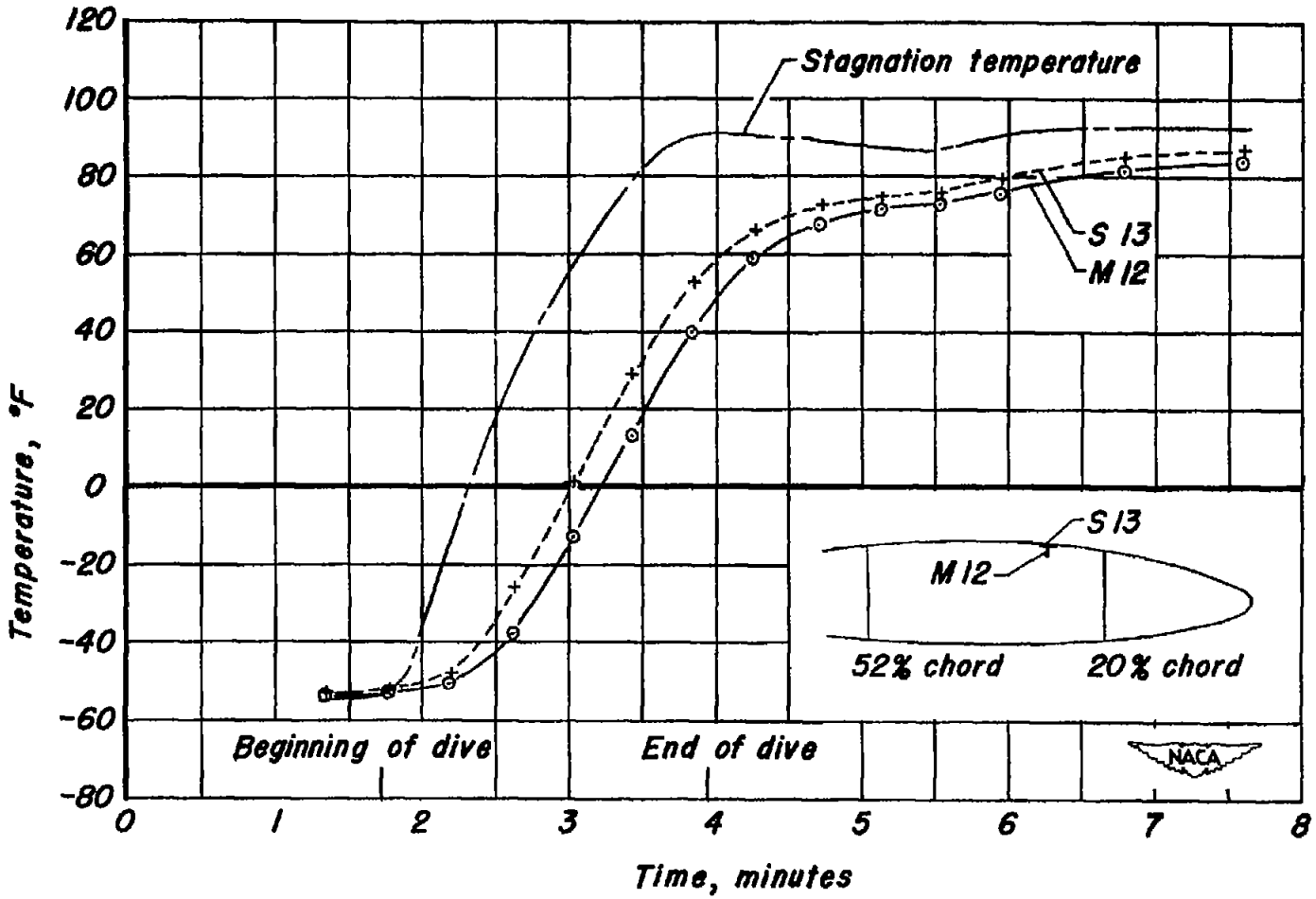


(a) Flight I, average rate of vertical descent 225 ft/sec

Figure 5.- Temperature difference between a typical skin-stiffener combination. Station 76 right wing.

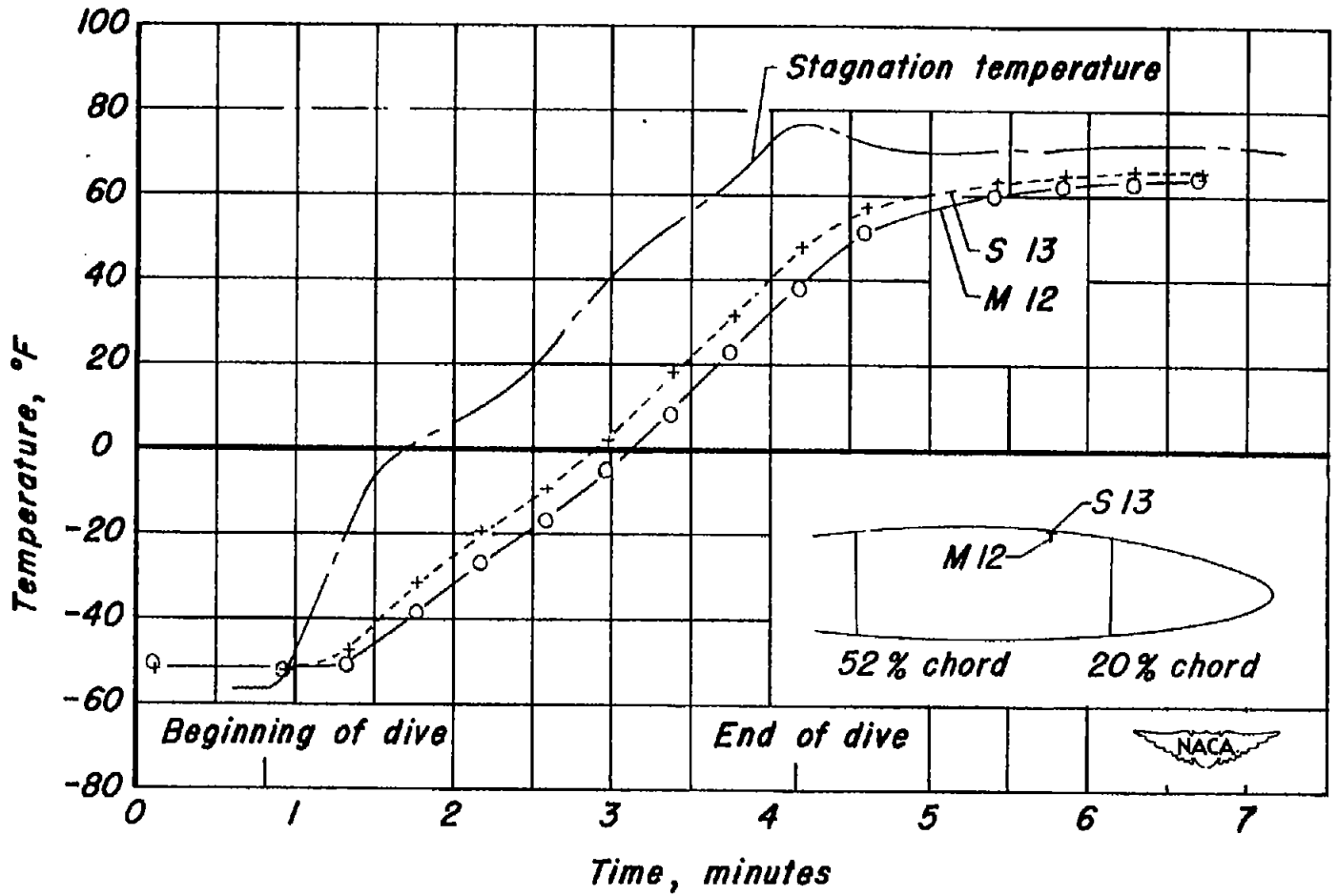


(b) Flight 2, average rate of vertical descent 150 ft/sec

Figure 5.- Continued.

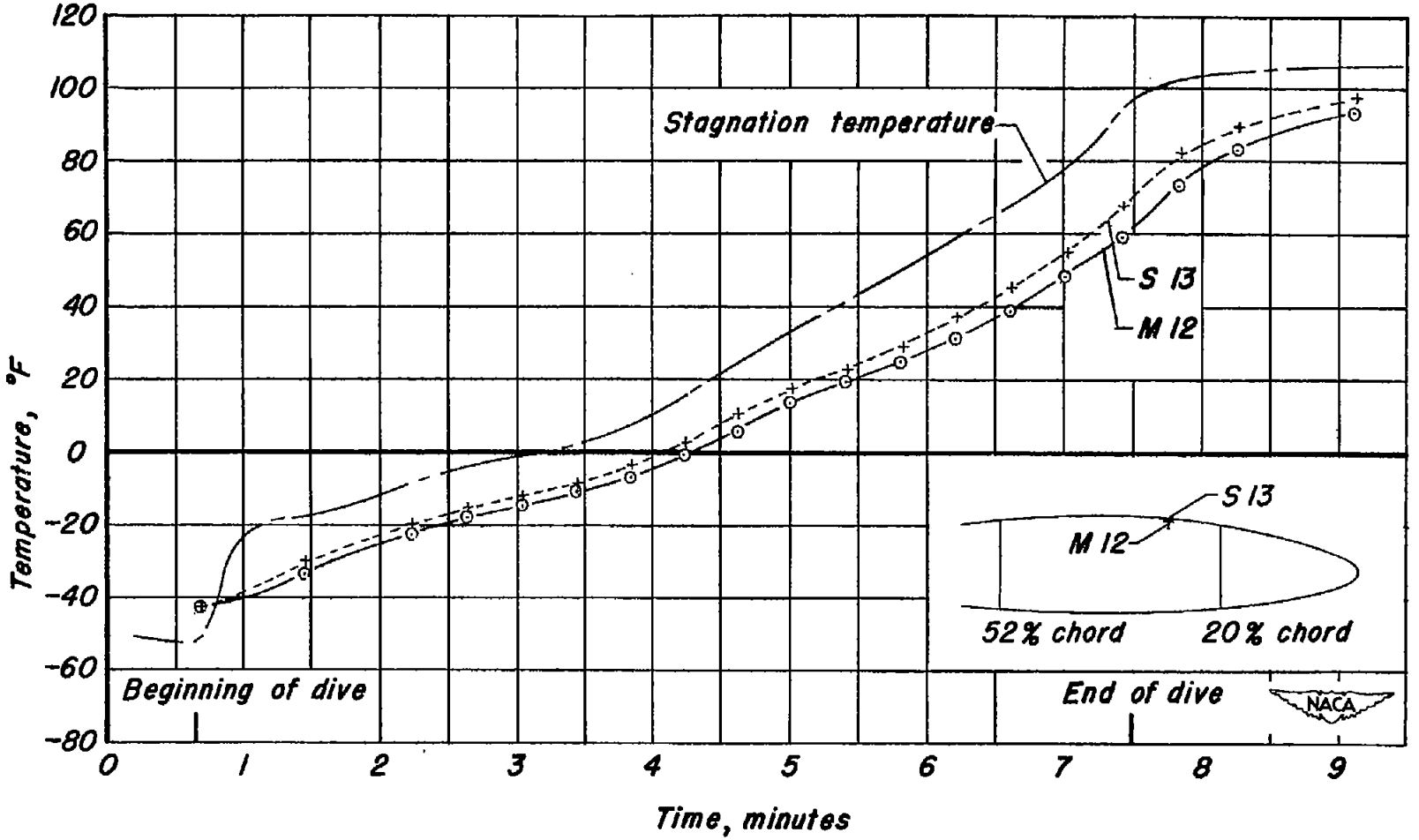


(c) Flight 3, average rate of vertical descent 73 ft/sec

Figure 5.- Concluded.

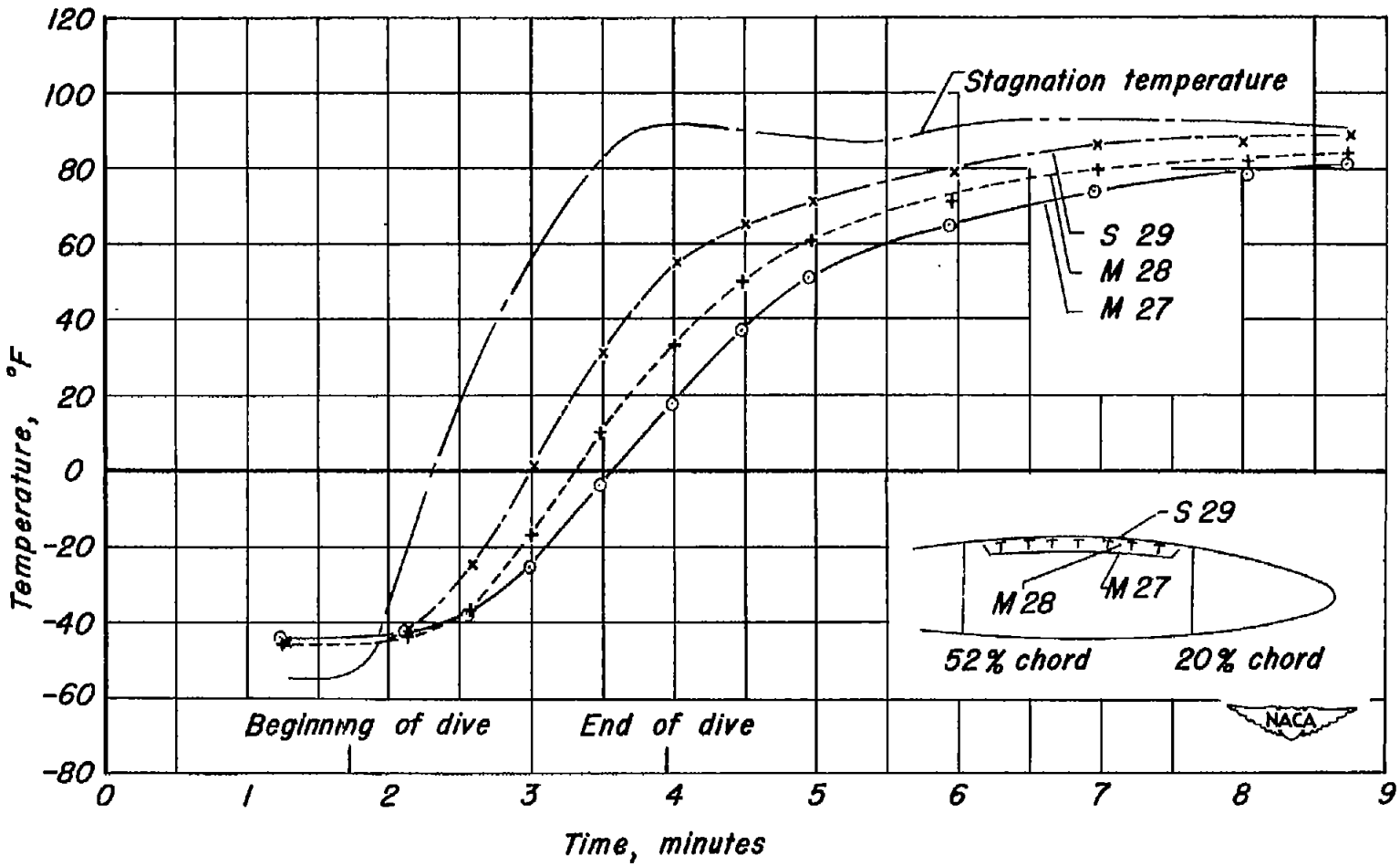


(a) Flight 1, average rate of vertical descent 225 ft/sec

Figure 6.– Temperature differences between the skin and a former at station 71.2 in right wing.

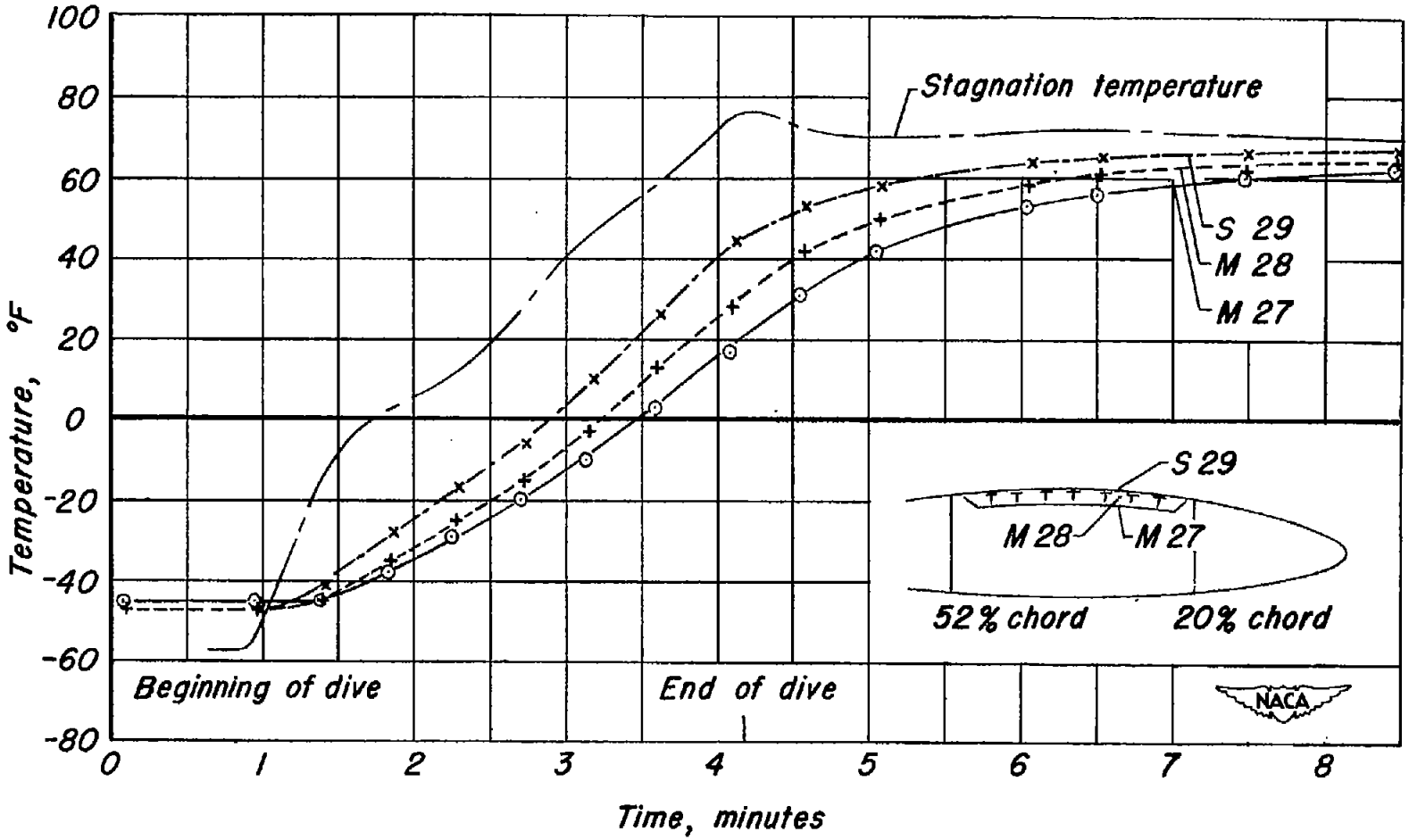


(b) Flight 2, average rate of vertical descent 150 ft/sec.

Figure 6.- Continued.

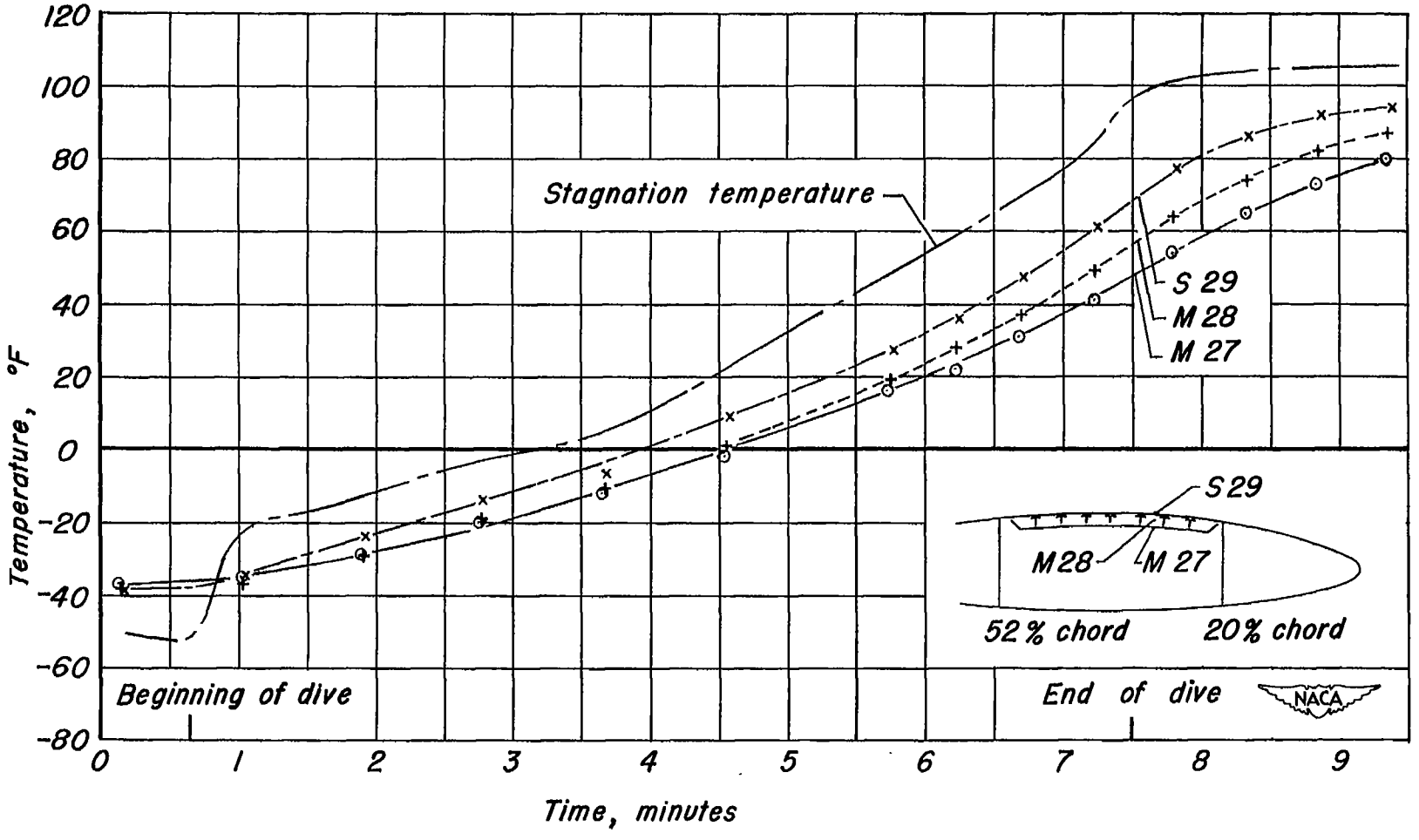


(c) Flight 3, average rate of vertical descent 73 ft/sec

Figure 6- Concluded.

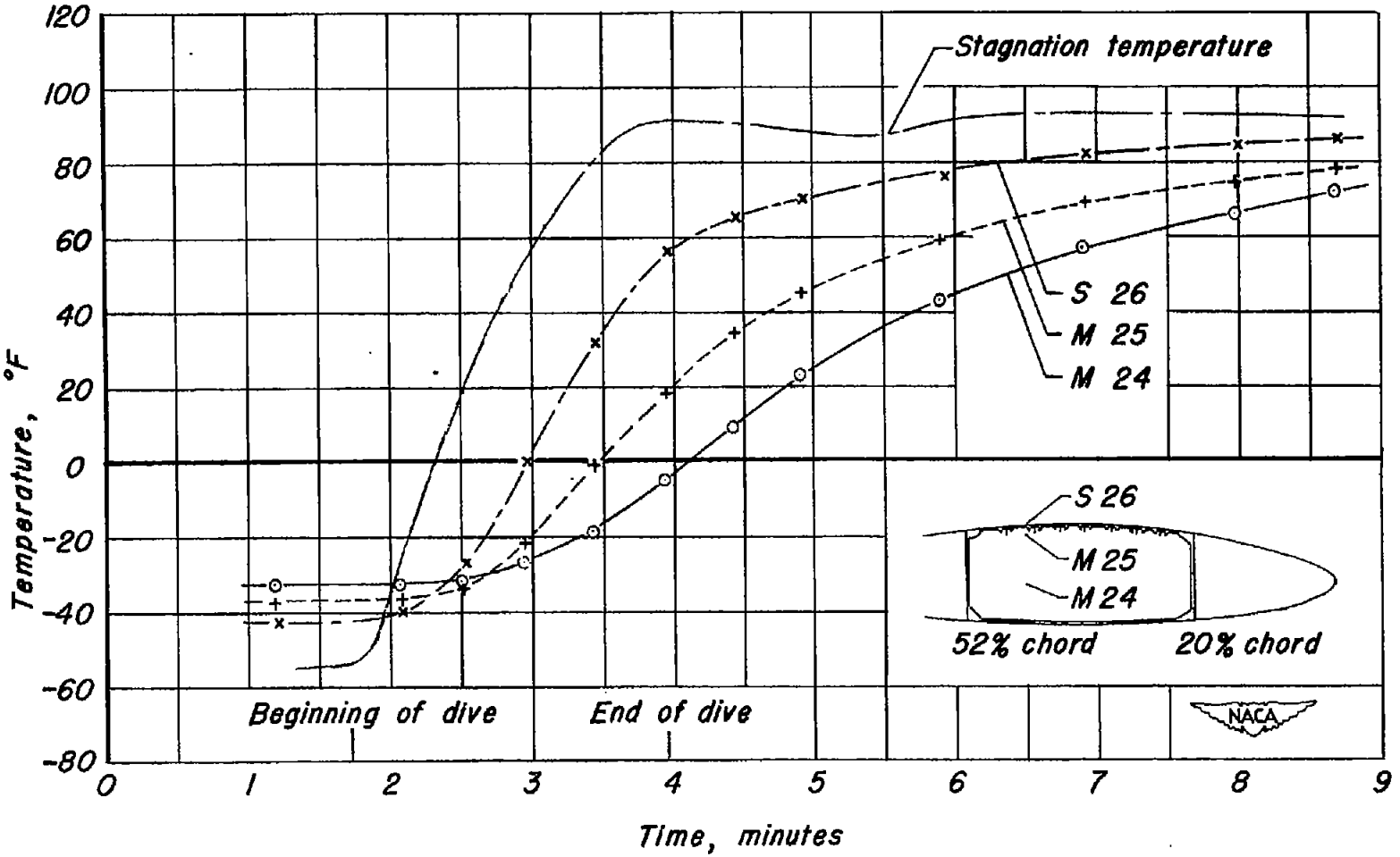


(a) Flight I, average rate of vertical descent 225 ft/sec

Figure 7.- Temperature differences across a rib at station 126 in right wing.

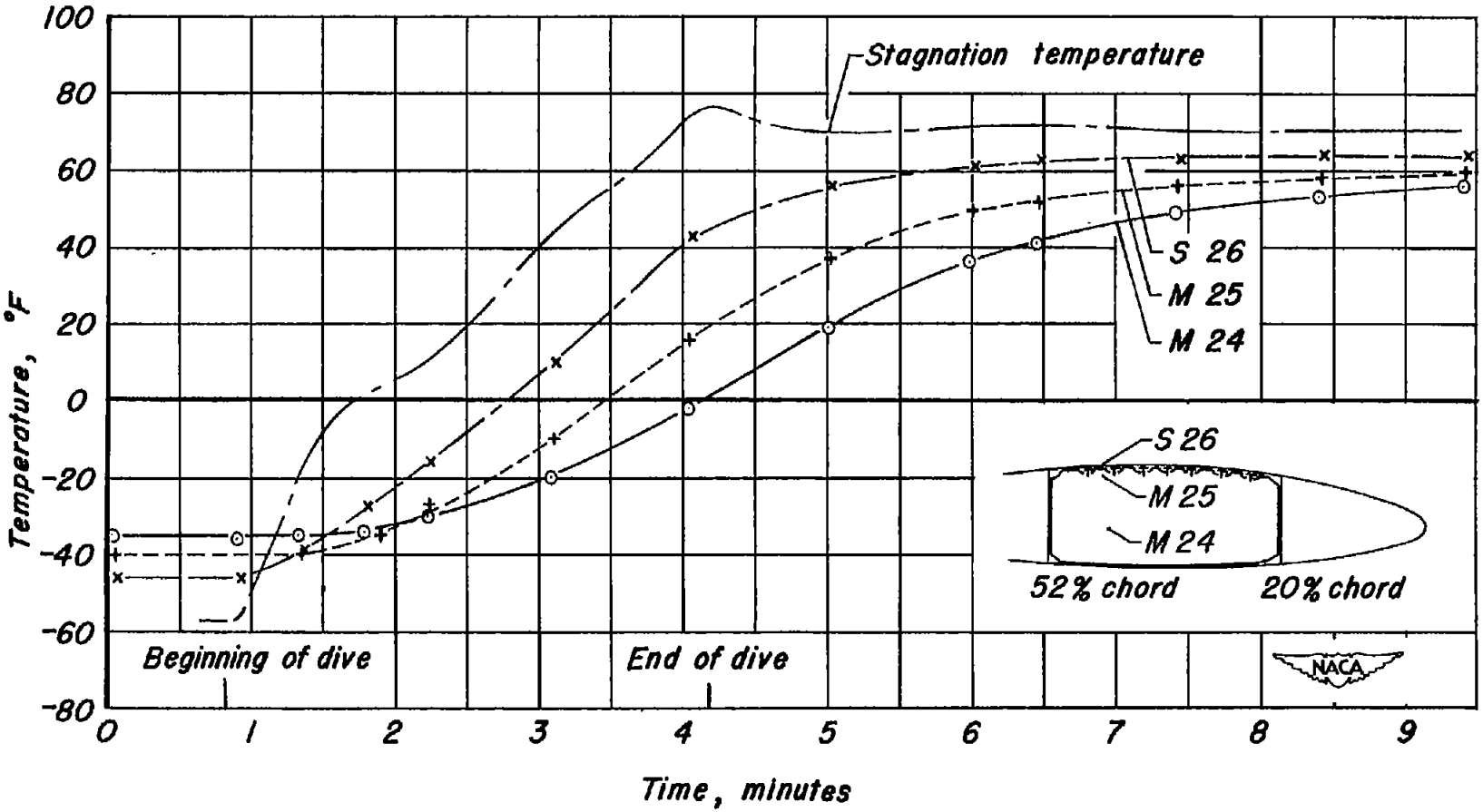


(b) Flight 2, average rate of vertical descent 150 ft/sec

Figure 7.– Continued.

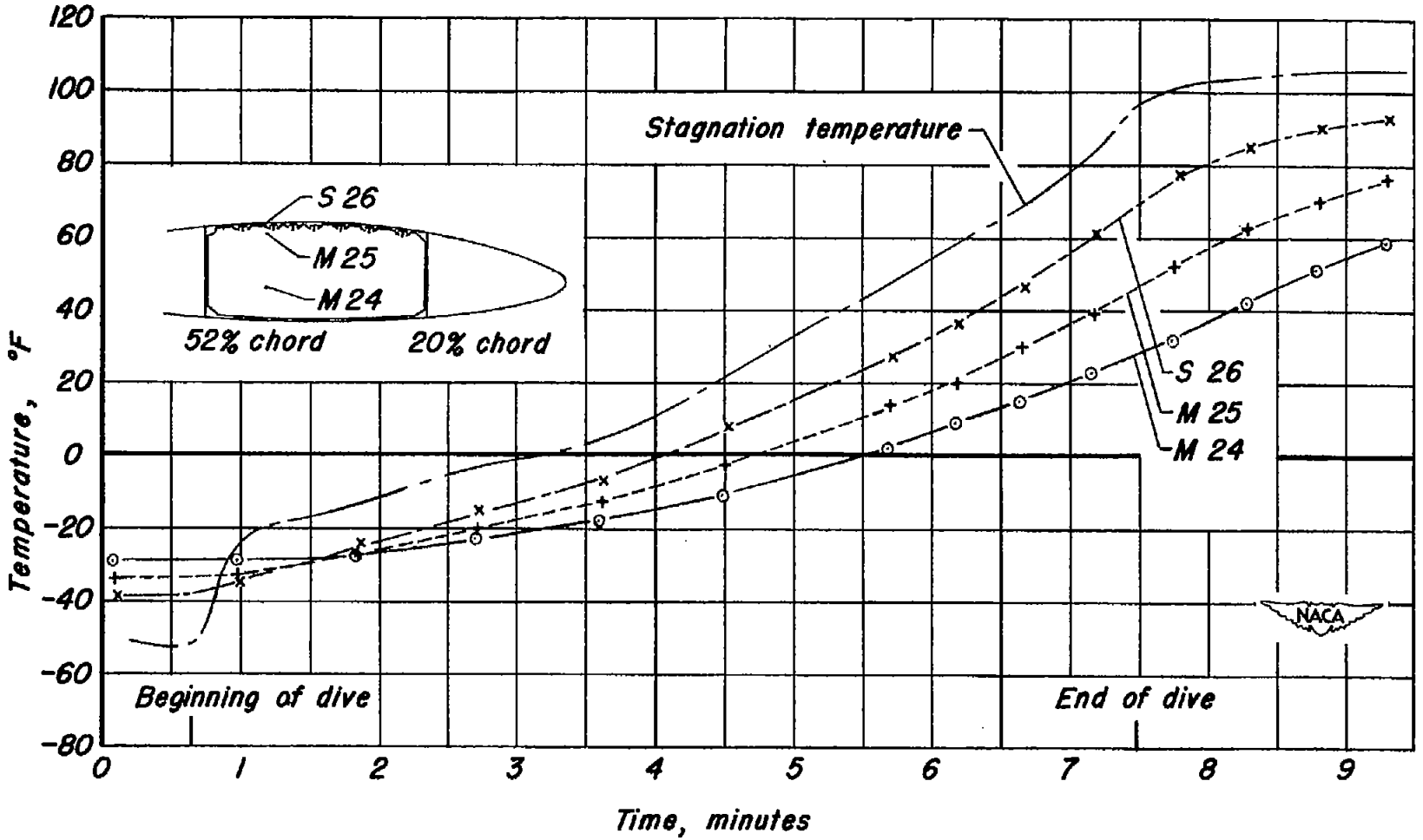


(c) Flight 3, average rate of vertical descent 73 ft/sec

Figure 7.- Concluded.

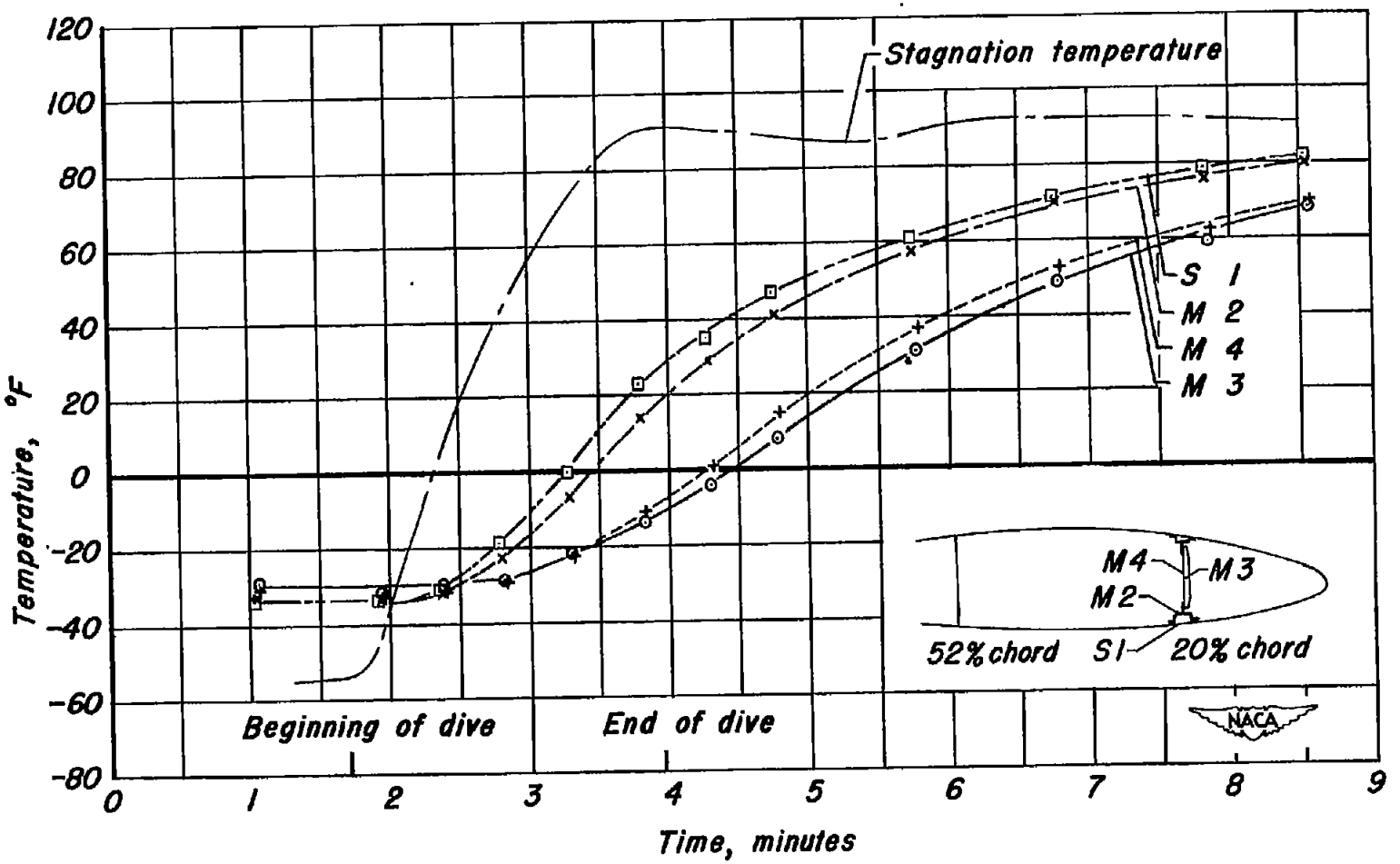


(a) Flight 1, average rate of vertical descent 225 ft/sec

Figure 8.- Temperature differences between the spar cap and the spar web at the 20 percent chord. Station 76 in right wing.

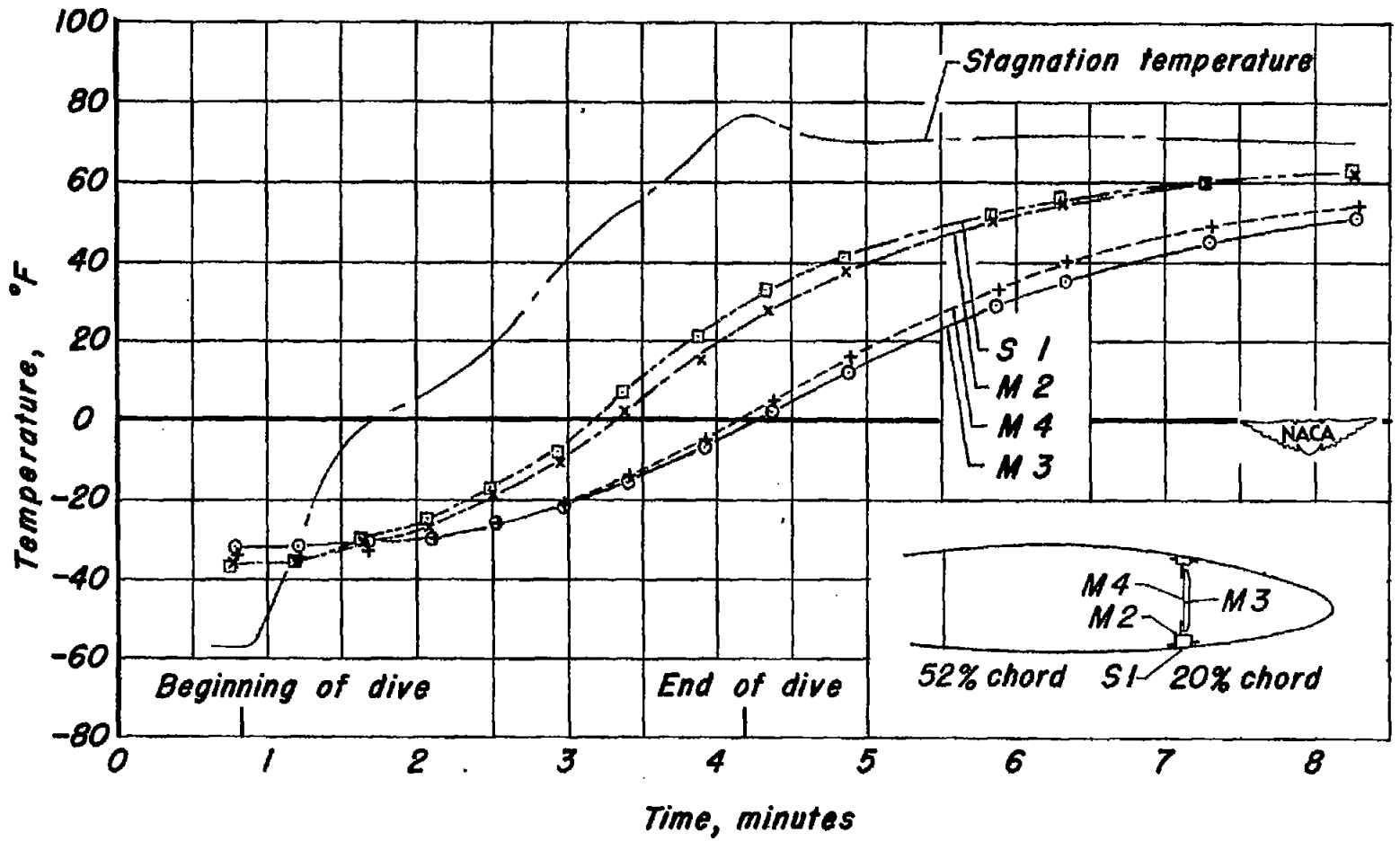


(b) Flight 2, average rate of vertical descent 150 ft/sec

Figure 8.- Continued.

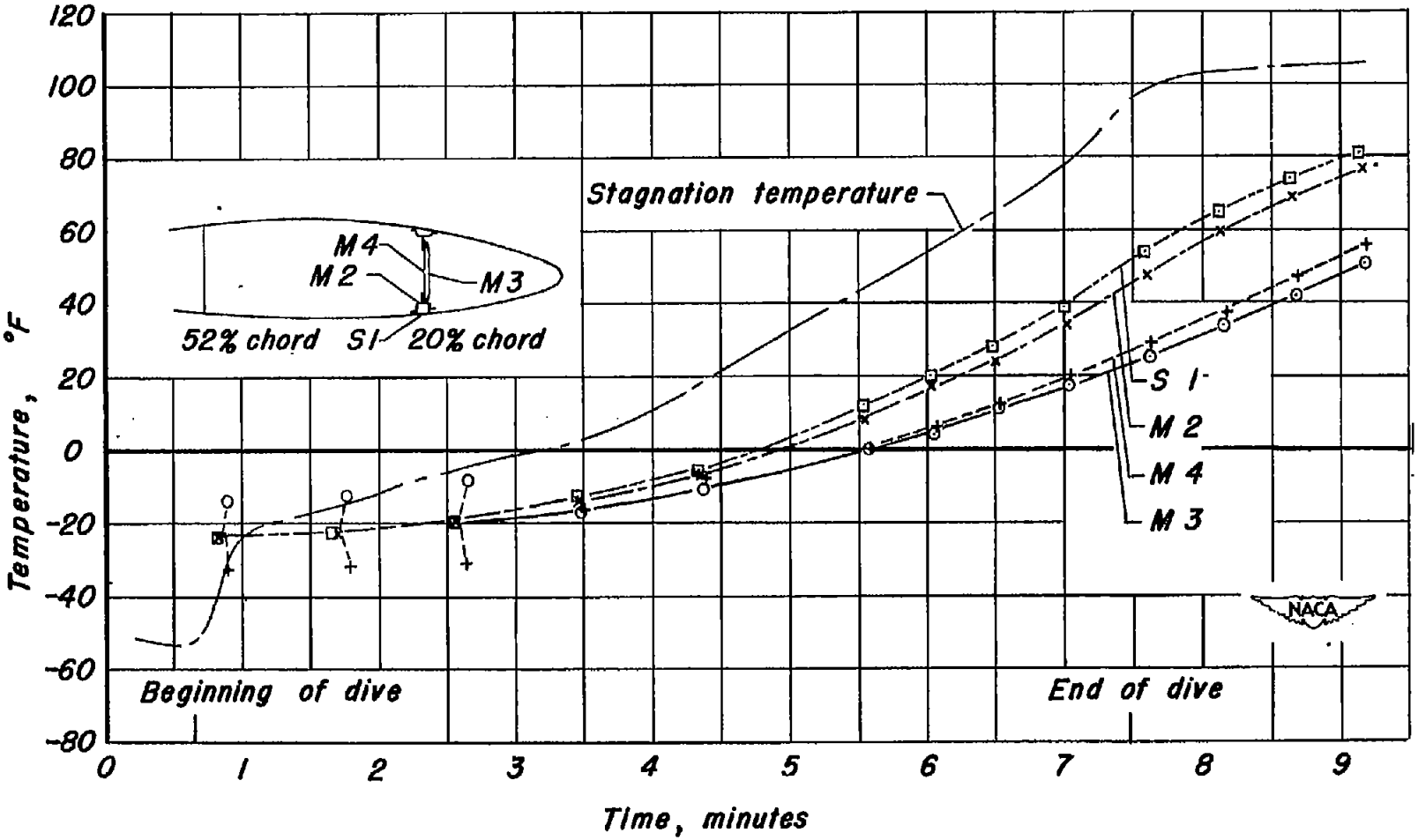


(c) Flight 3, average rate of vertical descent 73 ft/sec

Figure 8.- Concluded.

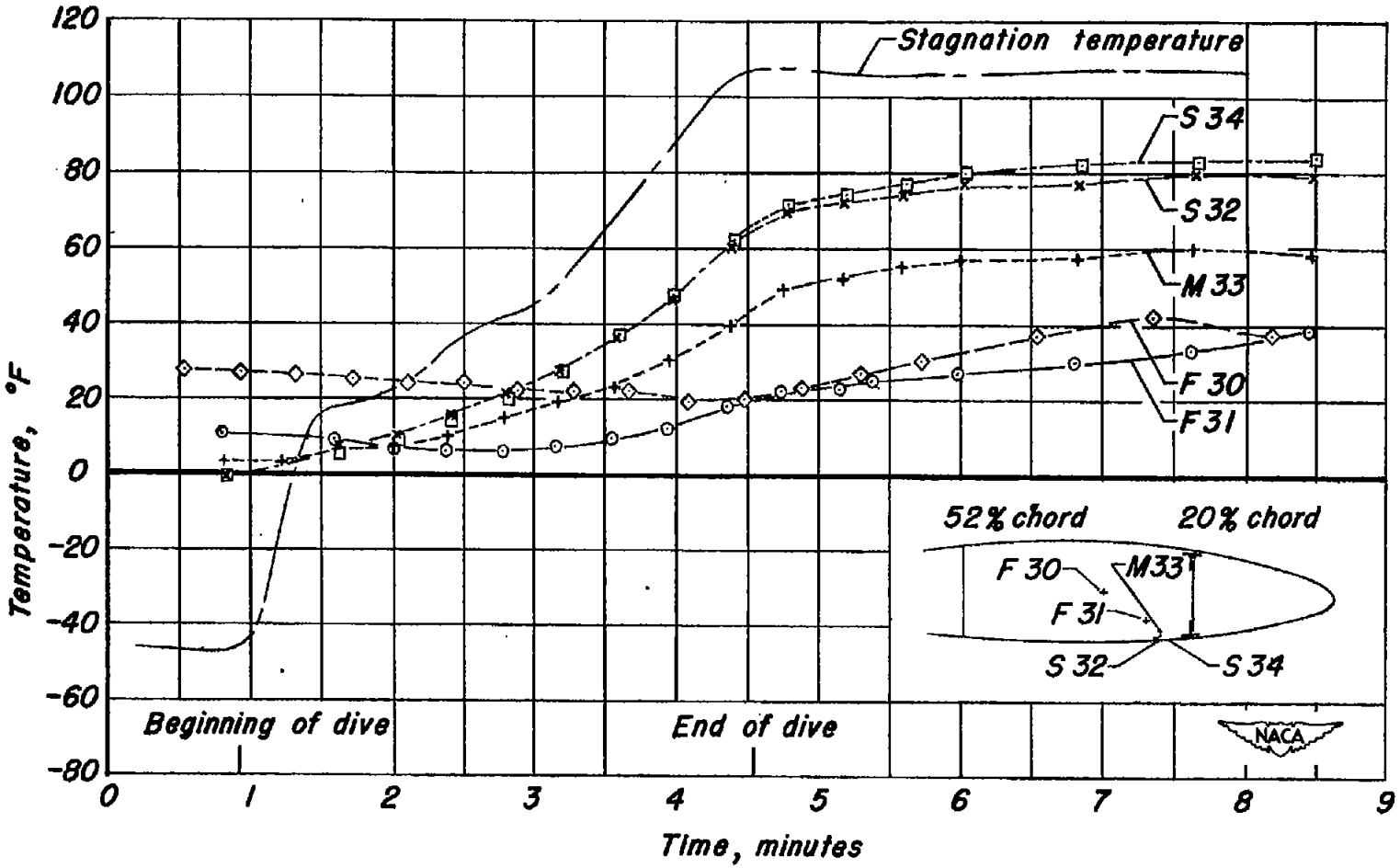


Flight 4, average rate of vertical descent 138 ft/sec.

Figure 9.- Temperature of the fuel and of the structure comprising the fuel tank at station 153 in right wing.

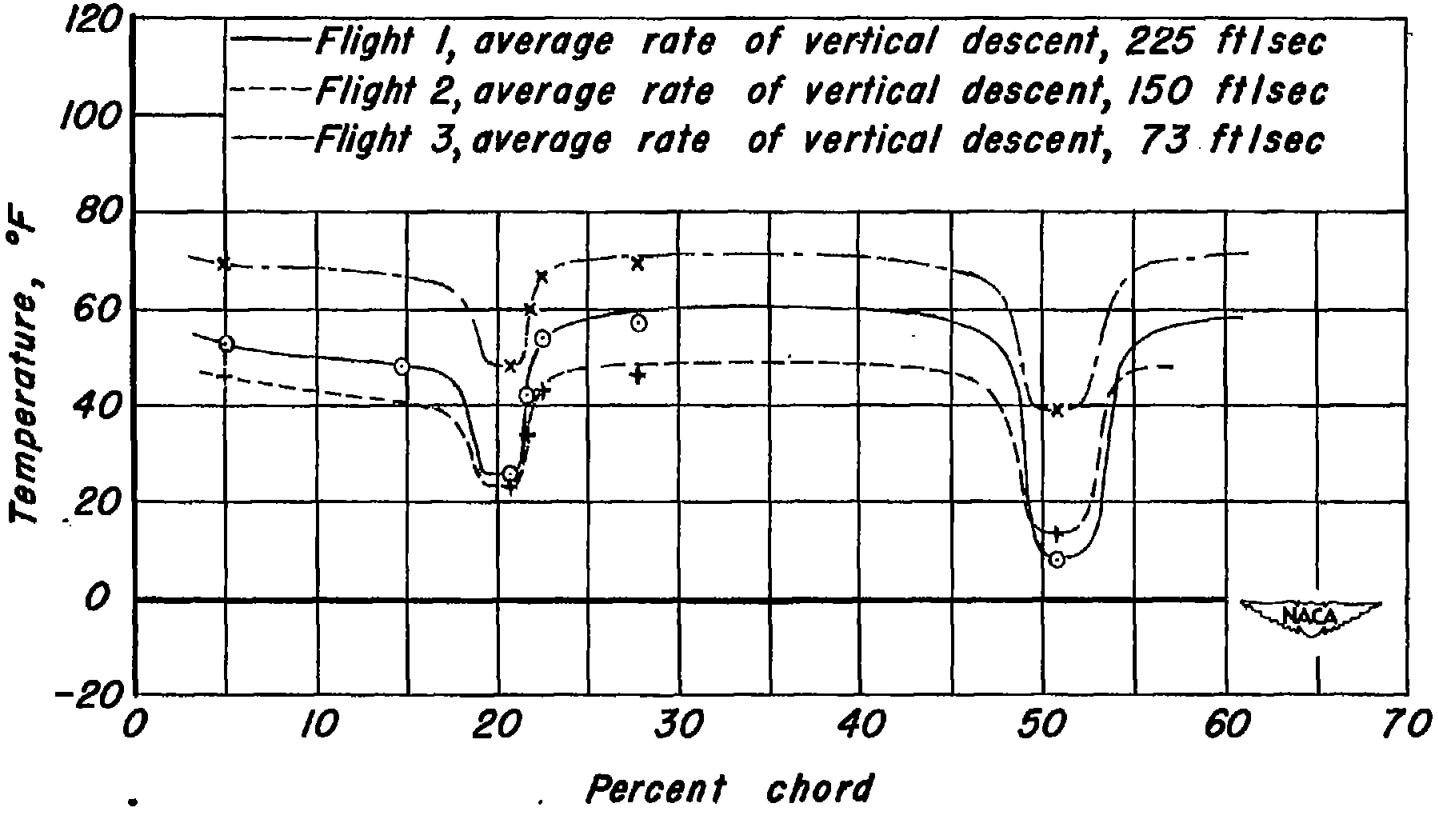


*Figure 10.- Chordwise temperature distribution at the termination of the dive. Station 76, upper surface of right wing.*

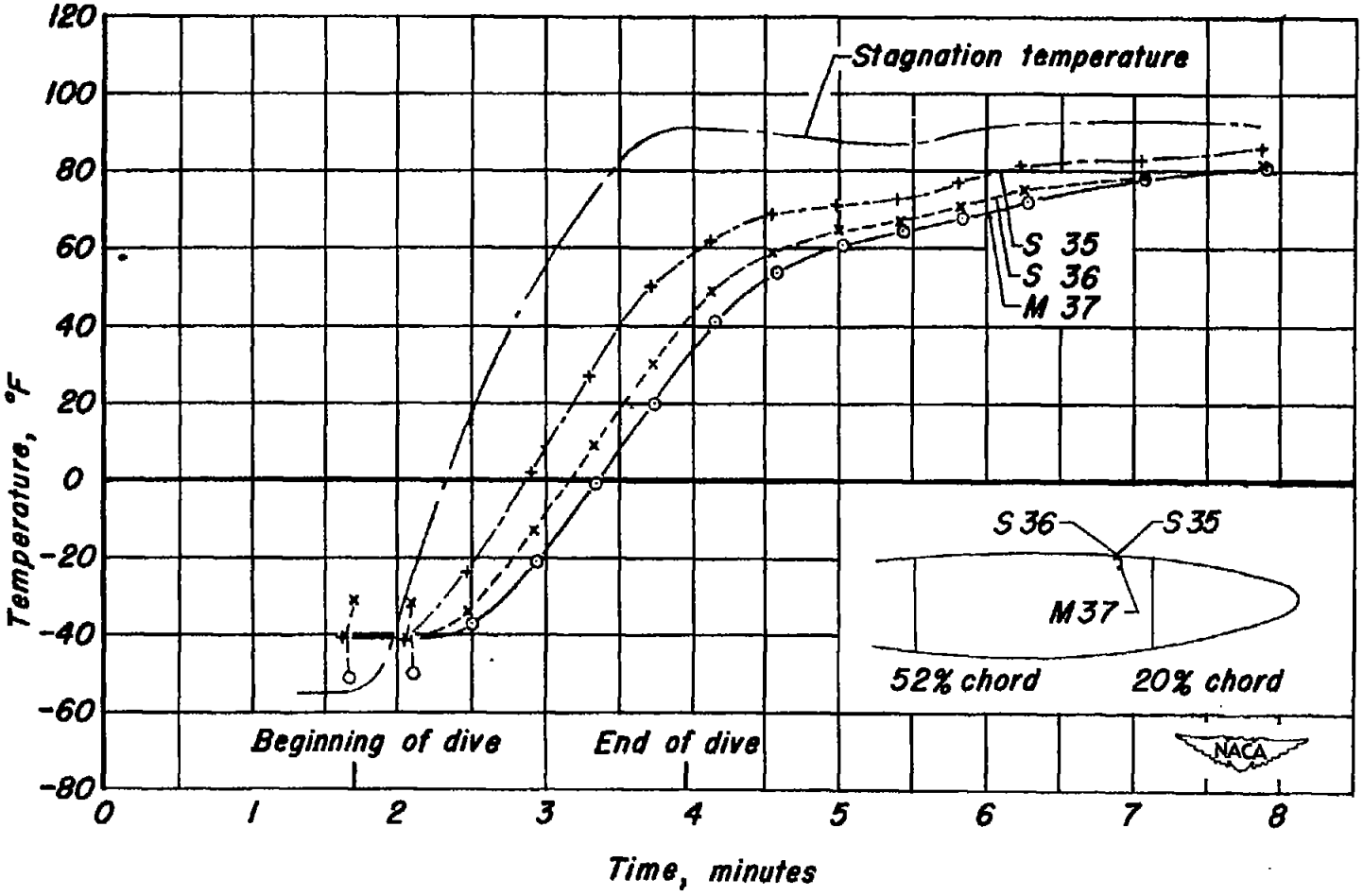


Flight I, average rate of vertical descent 225 ft/sec

Figure 11.- Temperature lag of the structure resulting from thick layers of paint on the wing surface at station 112 in left wing.

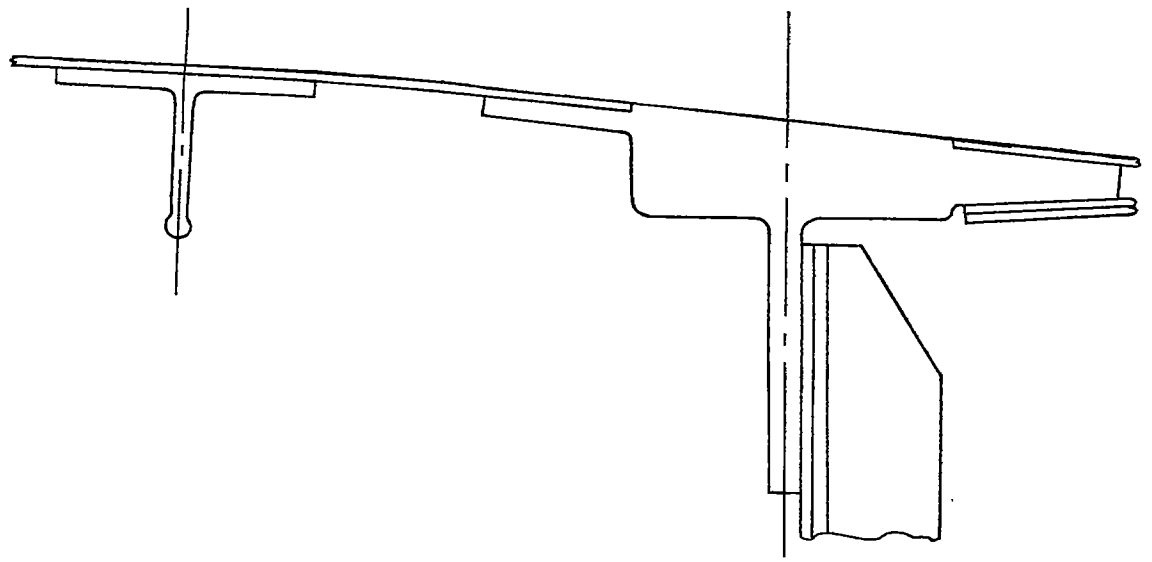

(a) Arrangement on test airplane

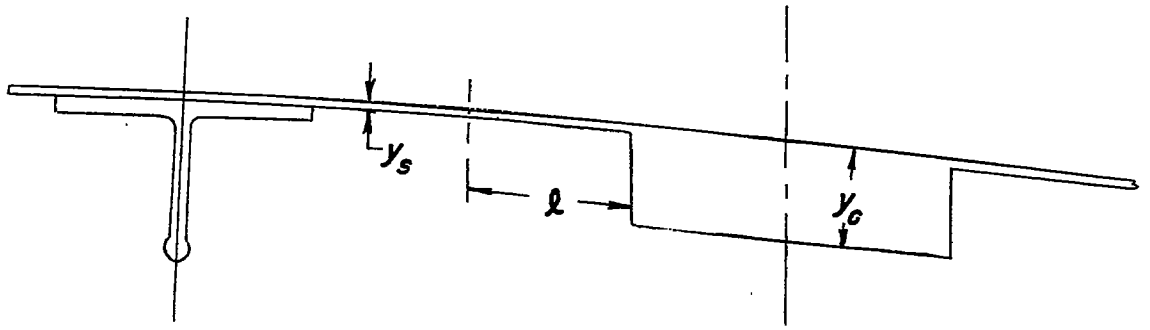


(b) Idealized arrangement

Figure 12.- Sketch of the skin and spar-cap to illustrate the method of calculating the skin and spar-cap temperatures.

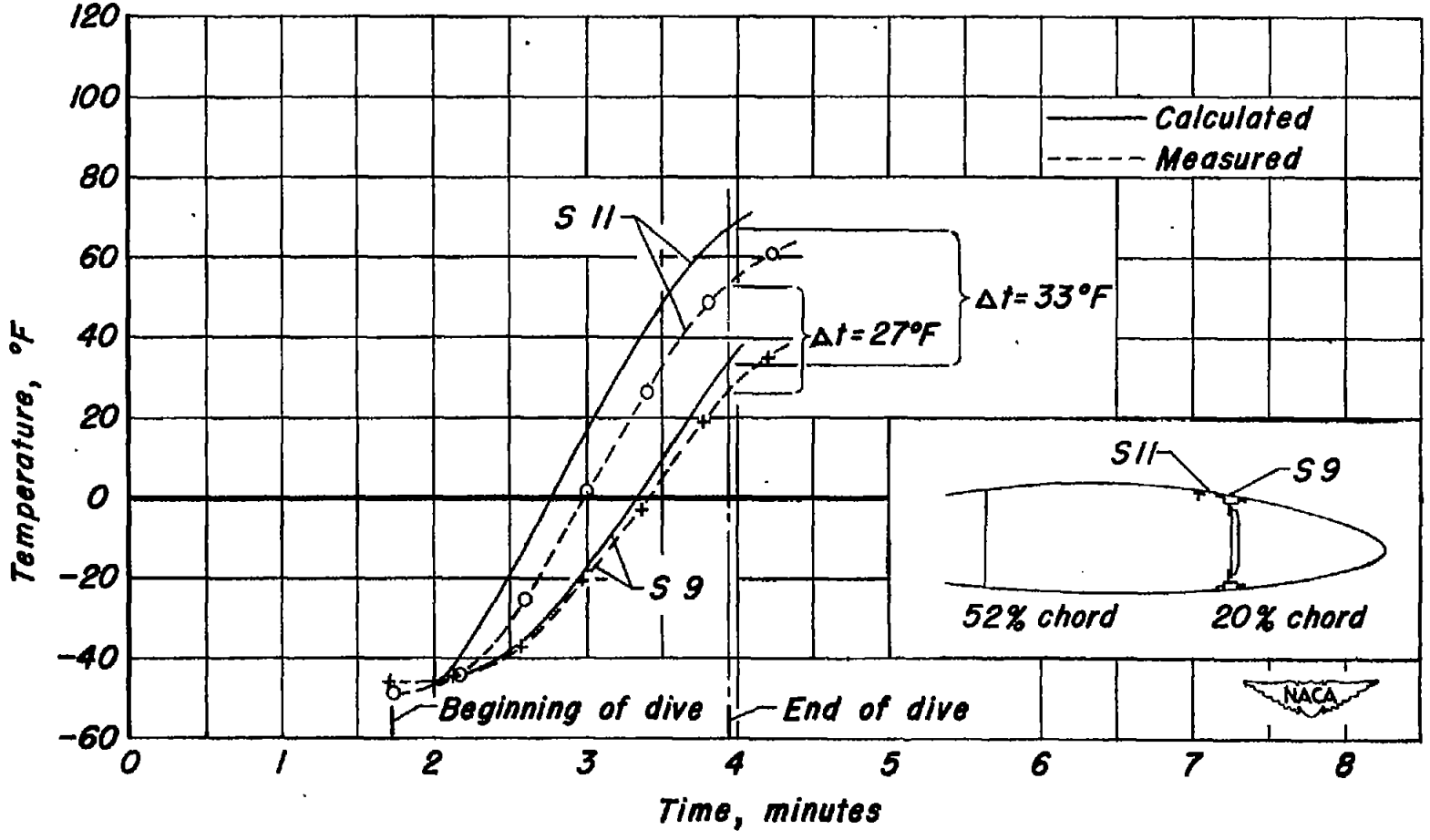


(a) Flight I, rate of vertical descent, 225 ft/sec

Figure 13.- Comparison during the dive between the measured and calculated temperatures of the spar cap and the skin adjacent to the spar cap. Right wing upper surface at 20 percent chord, station 76.

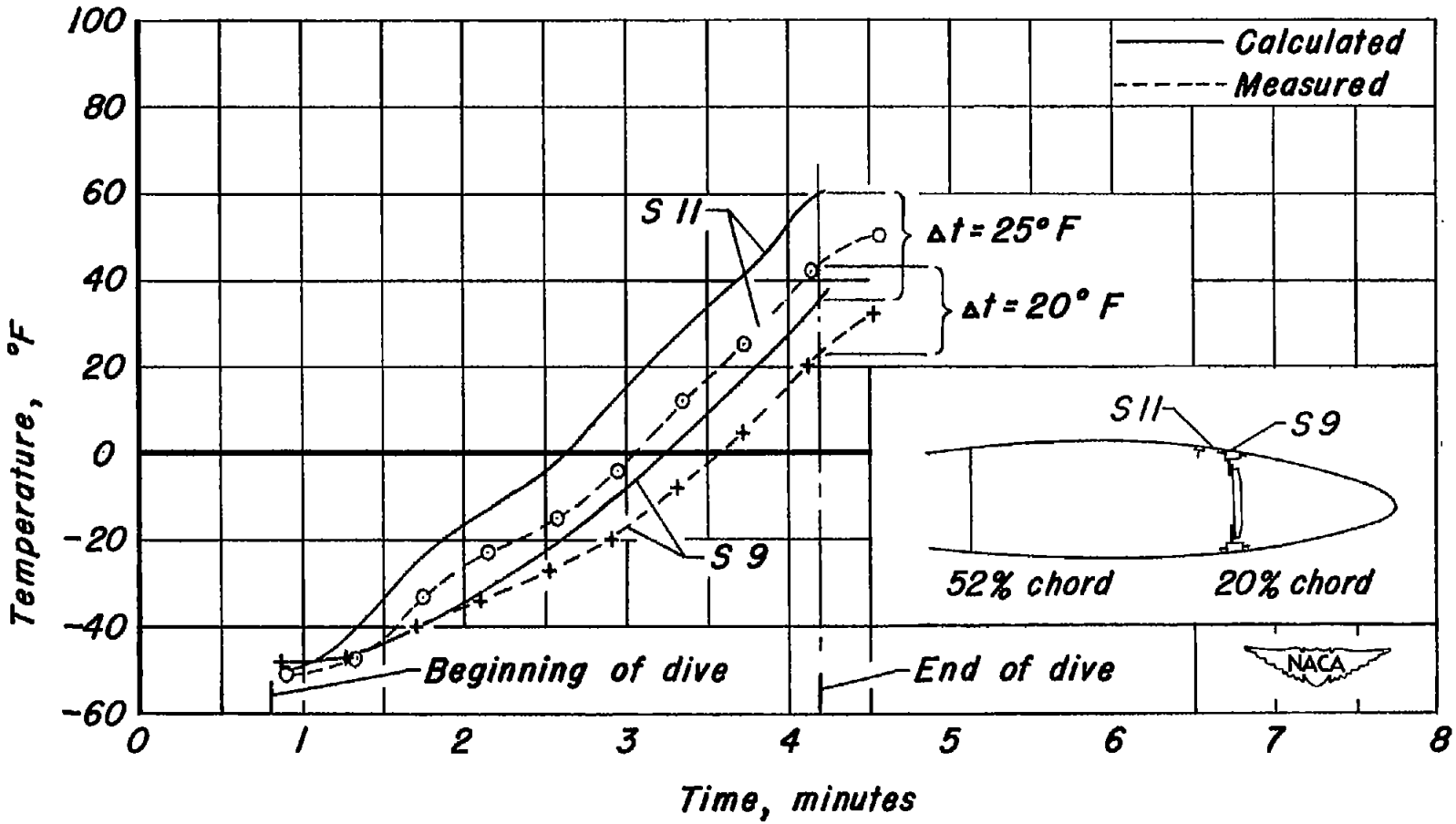


(b) Flight 2, rate of vertical descent 150 ft/sec

Figure 13.- Continued.

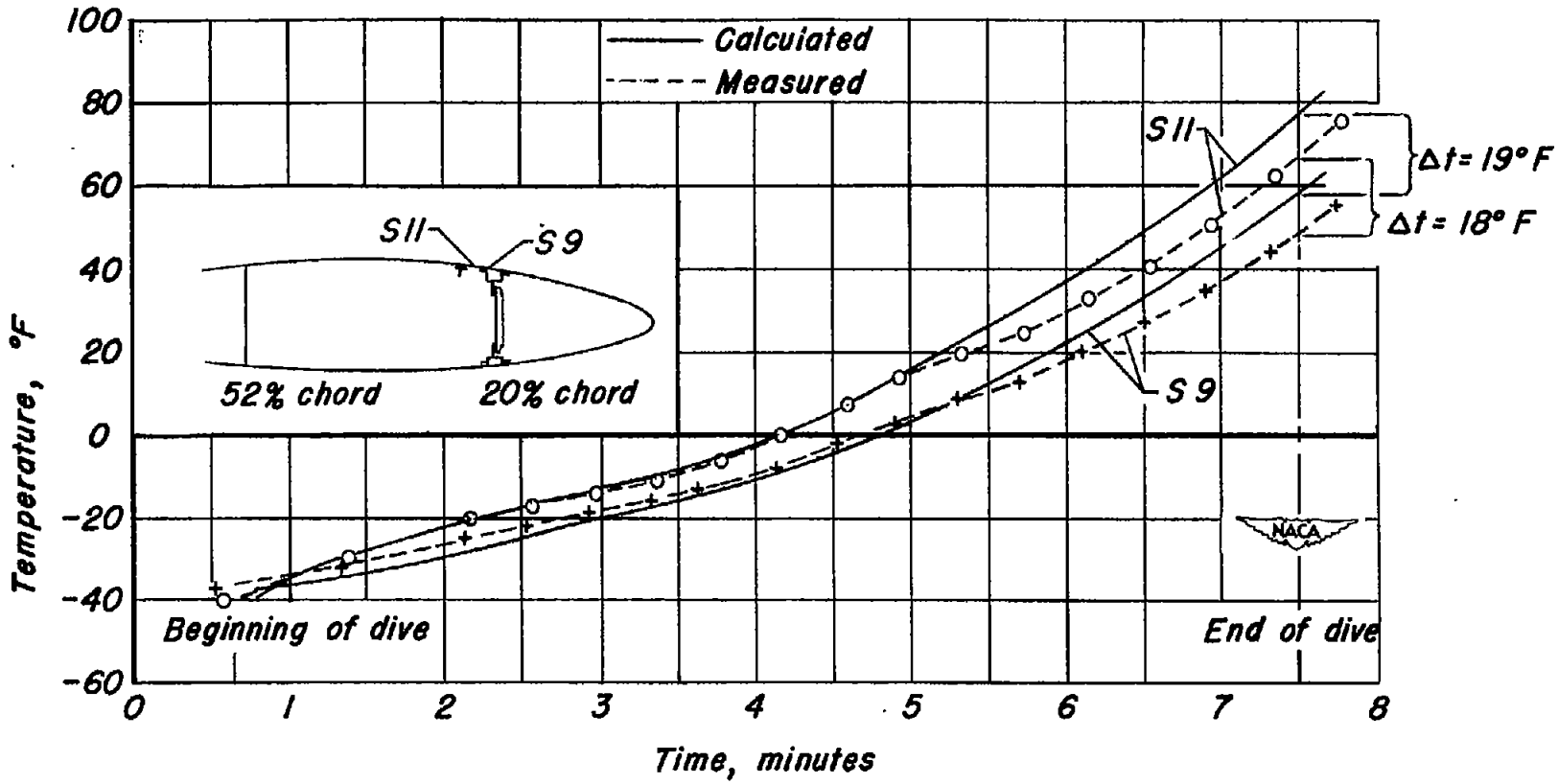


(c) Flight 3, rate of vertical descent 73 ft/sec

Figure 13.- Concluded.

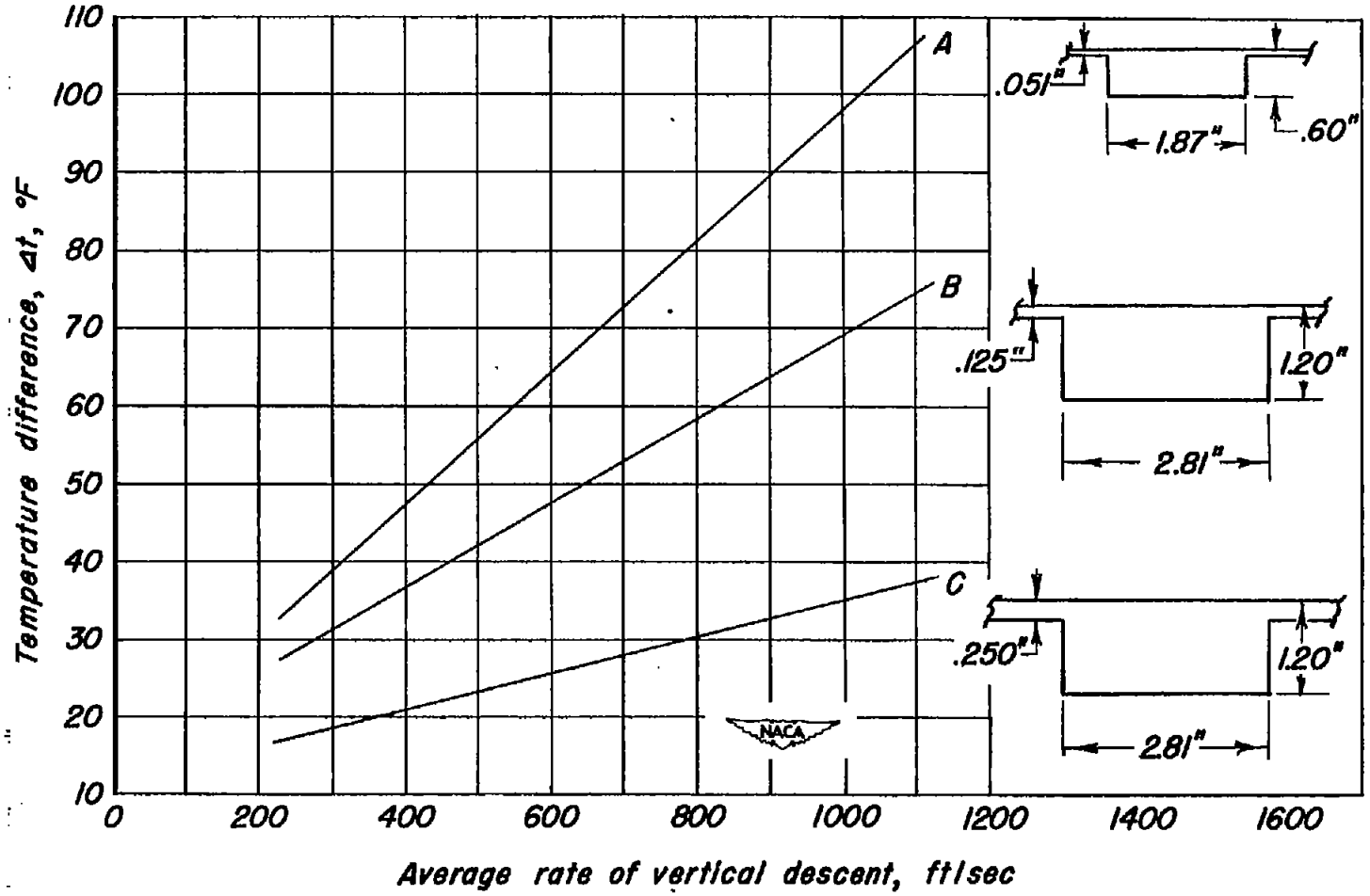


*Figure 14.- The calculated temperature differences between the skin and the spar cap for assumed arrangements at the termination of a dive from 35,000 feet to 5,000 feet, at various rates of vertical descent.*

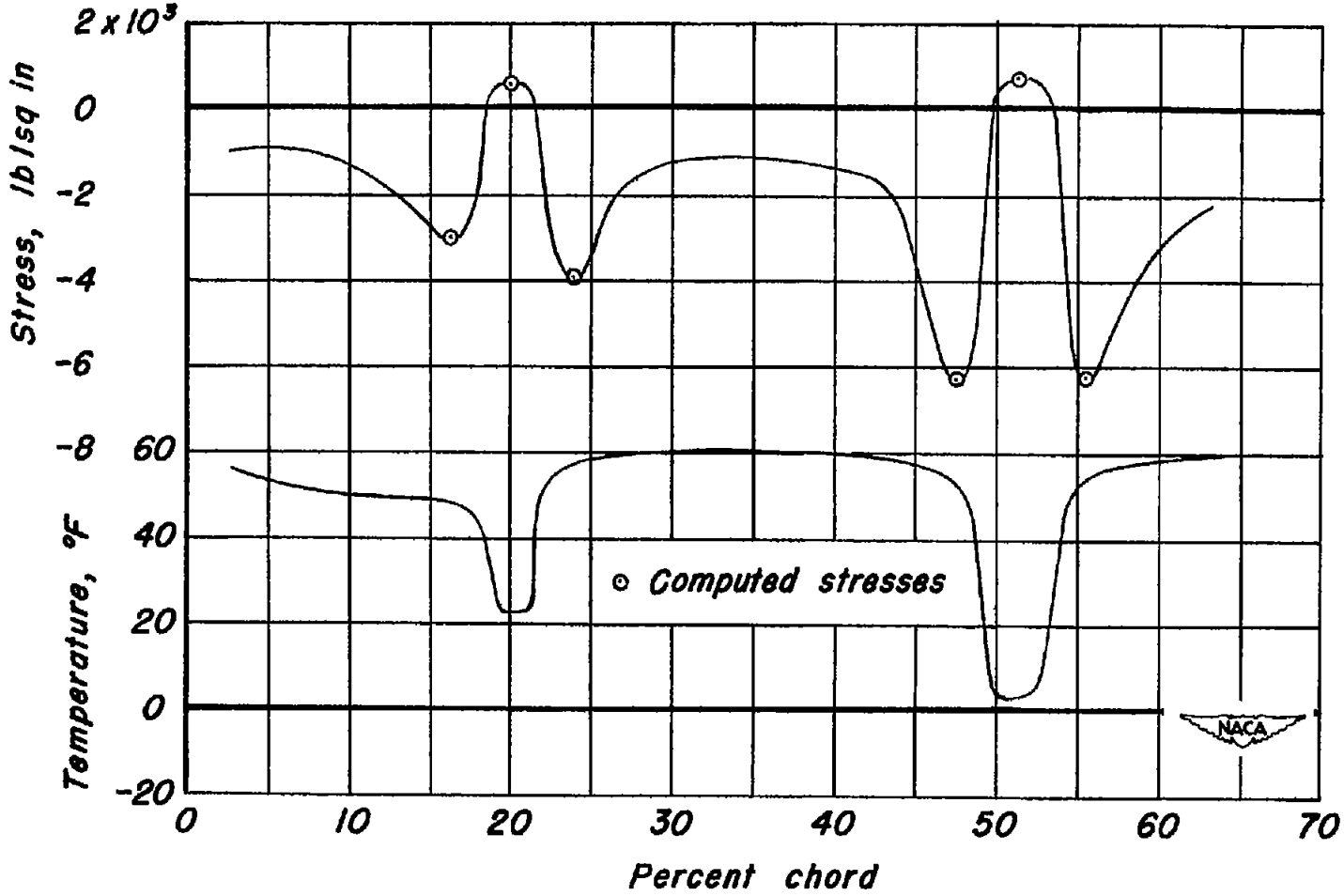


*Figure 15.- Predicted stresses induced in the wing as a result of the chordwise temperature distribution at the termination of the dive. Flight 1: station 76 right wing, upper surface.*